TERAHERTZ RADIATION GENERATION.

Accelerator-based THz sources

Mikhail Krasilnikov
Photo Injector Test facility at DESY in Zeuthen (PITZ)

25.06.2025, 13th MT ARD ST3 Meeting, DESY, Zeuthen

HELMHOLTZ

THz radiation

Parameter space

Applications

Methods of generation

DESY.

Introduction to Terahertz (THz) Radiation

Key points and challenges

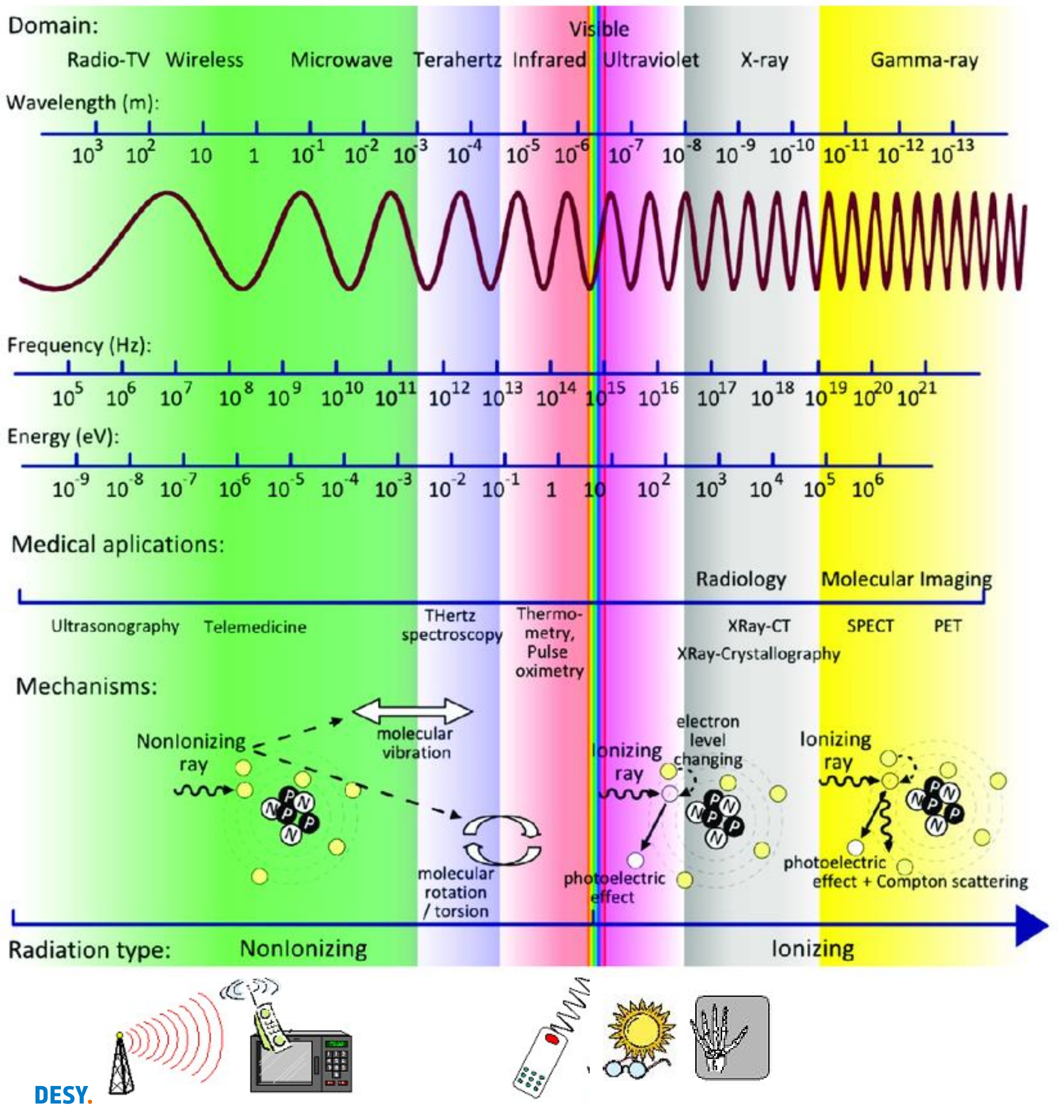

Terahertz Radiation:

- Frequency range: ~0.1 – 10 THz (~10 - 0.1 ps)
- Wavelength: ~30 μm - 3 mm (E~0.41 - 41.4 meV, T~4.8 – 478 K)

Phenomena at picosecond time scale

- Orbiting of electrons in highly-excited atomic states
- Rotation of small molecules
- Vibration of important collective modes of proteins
- Resonant frequencies of electrons in semiconductor and their nanostructures
- Superconducting energy gaps

Applications:

- Non-invasive imaging (biomedical, security)
- Spectroscopy (molecular fingerprint region)
- High-speed wireless communication
- Material science and semiconductor testing

*Historically, the **"THz gap"** refers to a frequency range where conventional electronic devices (effective for radio and microwaves) and photonic technologies (used for infrared and optical light) both perform poorly. This made terahertz radiation difficult to generate and detect, slowing progress in scientific and technological applications within this spectral region.*

"Standalone" Applications of THz Radiation

Imaging and Security Scanning

- THz waves have relatively low photon energy compared to visible light or X rays. They don't cause damage to atomic structures (non ionizing).
- For non invasive imaging in medical diagnostics and material inspection.
- THz radiation can penetrate non metallic and non polar materials like clothing, plastics, and paper etc.
- Useful in security systems (e.g., airport body scanners)

THz imaging is employed in transport terminals to detect concealed objects such as weapons or illicit items -providing a safe, non-ionizing alternative to conventional X-ray screening.

https://www.laserfocusworld.com/test-measurement/article/14235398/terahertz-imaging-advances-toward-medical-diagnostics

Determine the extent and depth of a basal cell carcinoma tumor (a kind of skin cancer) non-invasively through reflectance mode THz imaging.

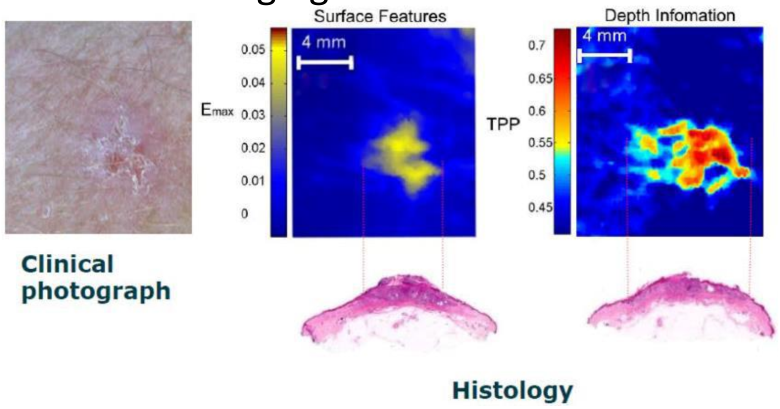

Taday, P.F.; Pepper, M.; Arnone, D.D. Selected Applications of Terahertz Pulses in Medicine and Industry. Appl. Sci. 2022, 12, 6169. https://doi.org/10.3390/app12126169

Other (selected) applications:
- THz communications (6G-7G, 0.1-10THz, ~1Tbps)
- Detection of chemical and biological compounds (TDS)
- THz Acceleration of electron beams
- Matter manipulation with intense THz radiation

Pump-probe experiments at XFEL with THz radiation

Needs for a THz source

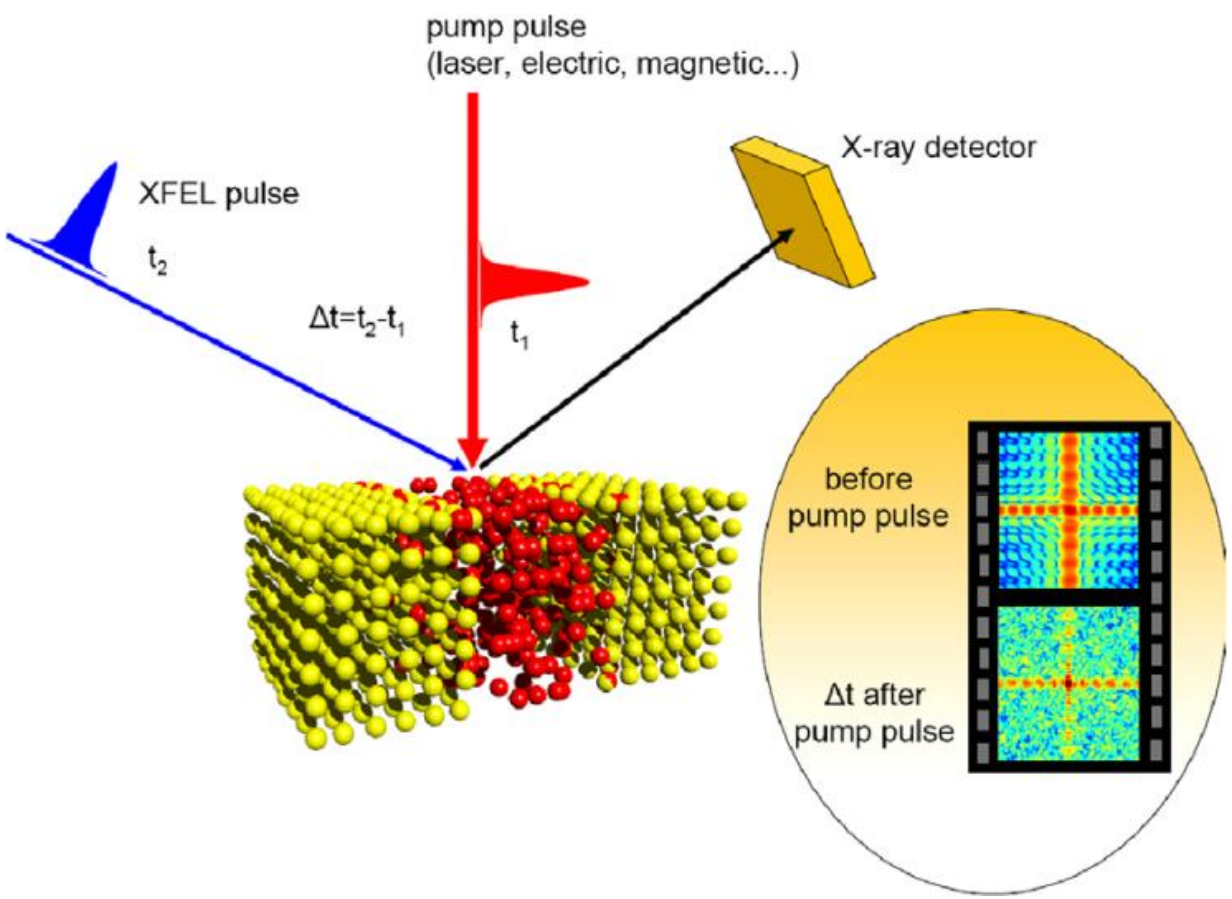

X-ray photon correlation spectroscopy (XPCS pump–probe technique)
G. Grübel et al. "XPCS at the European X-ray free-electron laser facility, Nucl. Instrum. and Methods B", 262, 357-367 (2007).

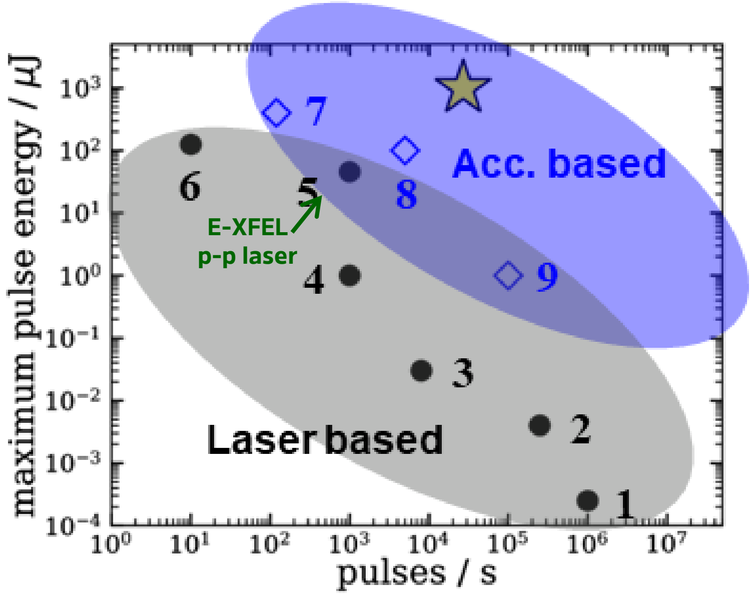

Laser based THz sources are limited at high repetition rate, while most IR/THz driven dynamics needs pulse energy above 1 μJ.

1,3,5,6 - Optical rectification [1]
2 - Photoconductive antenna [1]
4 - Two-color Laser filamentation [2]
7 - CTR (LCLS/FACET) [3]
8 - UR (FLASH) [4]
9 - UR (TELBE) [5]

[1] B. Green, et al, Sci.Rep.V. 6, Article number: 22256 (2016)
[2] M. Gensch, Proceedings of FEL 2013, 474 (2013)
[3] T. I. Oh et al 2013 New J. Phys. 15 075002
[4] https://flash.desy.de/
[5] https://www.hzdr.de/db/Cms?pOid=34100&pNid=2609&pLang=en

THz Generation Mechanisms

Laser-based	Accelerator-based	Plasma-based

Mechanism	Physical Principle	Typical THz Range	Advantages	Limitations	Applications
Photoconductive Antennas (PCA)	Ultrafast photoexcitation of carriers in a biased semiconductor	~0.1–3 THz	**Compact,** easy to operate; broadband	Low power (~nW–μW), cryogenic detectors may be needed	Imaging, spectroscopy, time-domain systems
Optical Rectification	Second-order nonlinear mixing in χ^2 crystals (e.g., ZnTe, GaP, $LiNbO_3$)	~0.1–5 THz	Broadband; **coherent** emission	Requires femtosecond lasers; low conversion efficiency, low rep. rate	THz-TDS, ultrafast material studies
Quantum Cascade Lasers (QCL)	Intersubband transitions in semiconductor superlattices	~1.5–5 THz	**CW**, **compact** chip-scale sources	Cryogenic cooling, limited tunability	THz sensing, imaging, spectroscopy
Free-Electron Lasers (FEL)	Synchrotron radiation from relativistic electrons in undulators	~0.1–100 THz	**Very high power (mW–W), tunable**	Large, expensive facilities	High-resolution spectroscopy, nonlinear THz science
Synchrotron Radiation	Bending radiation from electrons in storage rings	~0.1–10 THz	**Broadband, stable**	Large facility required, low repetition rate	Spectroscopy, material research
Accelerator-based Coherent THz (CSR/CTR)	Bunched relativistic electron beams (Coherent Synchrotron/Transition Radiation)	~0.1–10 THz	**High peak power; tunable via bunch length**	Large setup; requires beam diagnostics	THz FEL seeding, high-field experiments
Plasma-based Sources	Laser–plasma or beam–plasma interactions	~1–30 THz	**Ultra-short, high-field** pulses	Complex, often noisy; difficult to control	High-field THz, novel diagnostics
Difference Frequency Generation (DFG)	Nonlinear mixing of two optical fields in χ^2 media	~1–5 THz	**CW or pulsed**, wavelength **tunable**	Low conversion efficiency, requires phase matching	Spectroscopy, metrology
Spintronic THz Emitters	Ultrafast spin currents in ferromagnet/heavy metal layers	~0.1–10 THz	Simple design, broadband	Still experimental; moderate efficiency	Novel THz source research
Two-Color Laser Plasma	THz from asymmetric electron acceleration via ω–2ω laser pulses in air/gas plasma	~0.1–30 THz	Table-top, broadband, **single-cycle**	High laser power needed; low efficiency	Air plasma THz generation, ultrafast studies

THz source for pump-probe experiments at EuXFEL

THz source requirements (*P. Zalden, et al., "Terahertz Science at European XFEL", XFEL.EU TN-2018-001-01.0*)

- **Tunable** → $f = 0.1 \ldots 20\ THz\ (\lambda_{rad} = 3mm \ldots 15\mu m)$
- Various temporal and *spectral* patterns, polarization - ideally **narrow-band** → $^{\Delta W}/_{W} \sim 0.1 \ldots 0.01$
- Time jitter → from CEP (few fs) *stable* for field driven to "intensity" driven dynamics (~longest pulse duration) → $\sigma_t \sim {}^{0.1}/_{f}$
- **High pulse energy** $W > 10\mu J$ (μJ - hundreds of μJ - mJ , depending on f)
- **Repetition rate** to follow European XFEL → $(600\mu s \ldots 900\mu s) \times (0.1 \ldots 4.5MHz) \times 10Hz = 27000 \ldots 40500\ pulses/s$

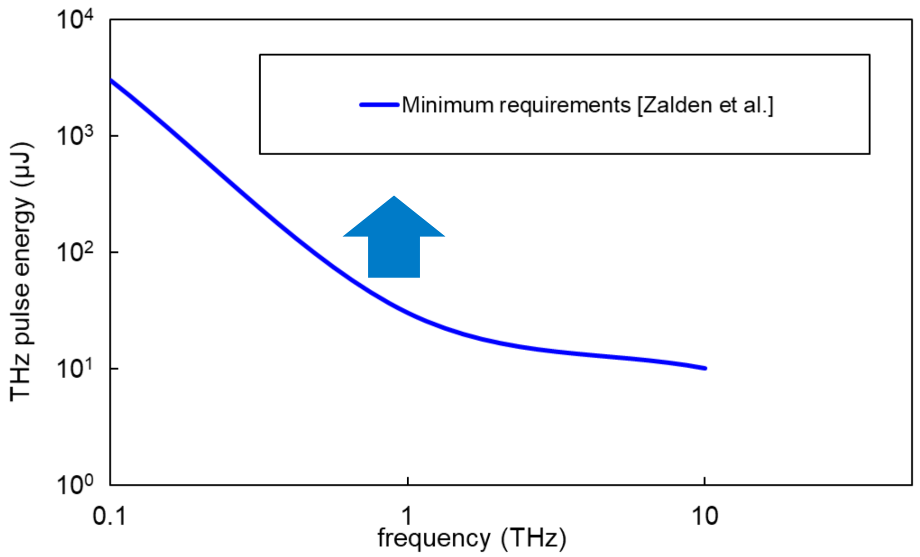

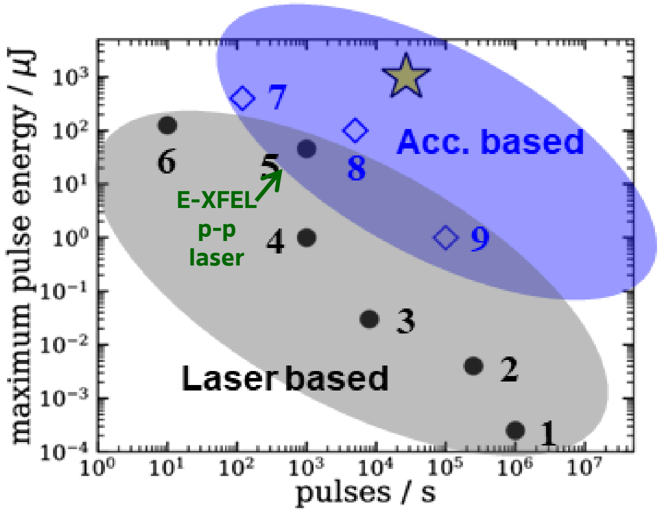

THz source for pump-probe experiments at XFEL

Accelerator-based THz sources

Generation of THz radiation by relativistic **electron beams**

Attractive features:

- clean in-vacuum radiation production
- tunability (electron beam manipulation)
- potential to provide high power (high field)
- polarization control

Methods of generation:

- bend magnet → CSR
- **transition / diffraction radiation (CTR/CDR)**
- **undulator → e.g., THz Free Electron Lasers (FELs)**
- Cherenkov radiation (DLW), corrugated structures
- Smith–Purcell radiation

Coherent Emission Basics:

- Coherence condition: When bunch (microbunch) length ≤ THz wavelength
- Power scaling: Coherent radiation $\propto N^2$ (number of electrons per bunch)
- Requires ultrashort / modulated, high-charge bunches → strong compression techniques and advanced beam shaping

Accelerator-based THz sources: CTR / CDR

Coherent Transition / Diffraction Radiation (CTR / CDR)

CTR:

Electron bunch hitting a **metallic foil**

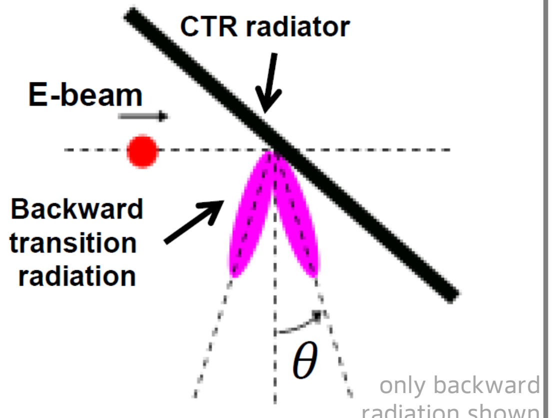

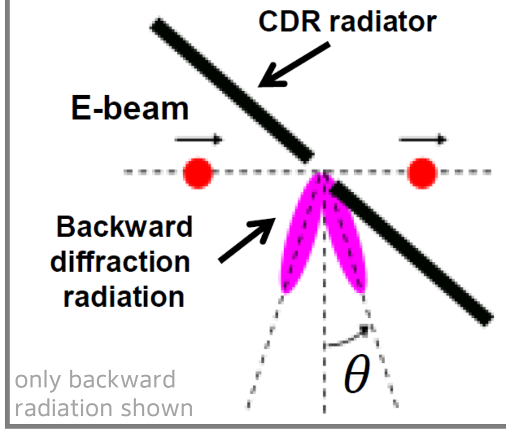

CDR:

Electron bunch passing **close to a metal screen with a hole / slit**

Backward TR energy emitted in the frequency range $d\omega$ into the solid angle $d\Omega$ can be calculated from the generalized Ginzburg-Frank Formula:

$$\frac{d^2U_e}{d\omega d\Omega} = \frac{e^2}{4\pi^3\varepsilon_0 c}\frac{\beta^2\sin^2\theta}{(1-\beta^2\cos^2\theta)^2}$$

The spectral and spatial radiation energy in the far-field regime:

$$\frac{d^2U_{\text{bunch}}}{d\omega d\Omega} = \frac{d^2U_e}{d\omega d\Omega}\cdot \boldsymbol{N^2}\left|F_{long}(\omega)\right|^2\cdot\left[\frac{2c}{\omega r_b\sin\theta}J_0\left(\frac{\omega r_b\sin\theta}{c}\right)-\frac{2c\beta\gamma}{\omega r_b}I_0\left(\frac{\omega r_b}{c\beta\gamma}\right)T(\gamma,\omega a,\theta)\right]^2$$

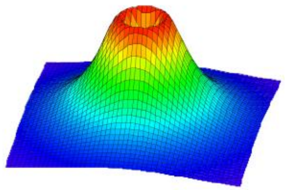

$$T(\gamma,\omega a,\theta) = \frac{\omega a}{c\beta\gamma}J_0\left(\frac{\omega a\sin\theta}{c}\right)K_1\left(\frac{\omega a}{c\beta\gamma}\right)+\frac{\omega a\sin\theta}{c\beta^2\gamma^2\sin\theta}J_1\left(\frac{\omega a\sin\theta}{c}\right)K_0\left(\frac{\omega a}{c\beta\gamma}\right)$$

Longitudinal Form factor of the e-beam

$$F_{long}(\omega) = \int_{-\infty}^{+\infty}\rho_{long}(t)e^{-i\omega t}dt$$

L.D. Landau, E.M. Lifshitz, "Electrodynamics of Continuous Media", Pergamon, New York, 1960
S.Casalbuoni et al., "Far-Infrared Transition and Diffraction Radiation", TESLA 2005-15

Accelerator-based THz sources: Undulator radiation

THz radiation from the undulator

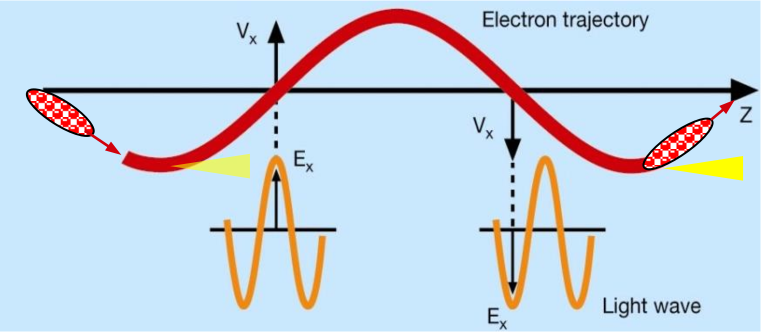

- Tunable narrowband THz source
- High brightness (especially for short, dense bunches → **coherent** THz)

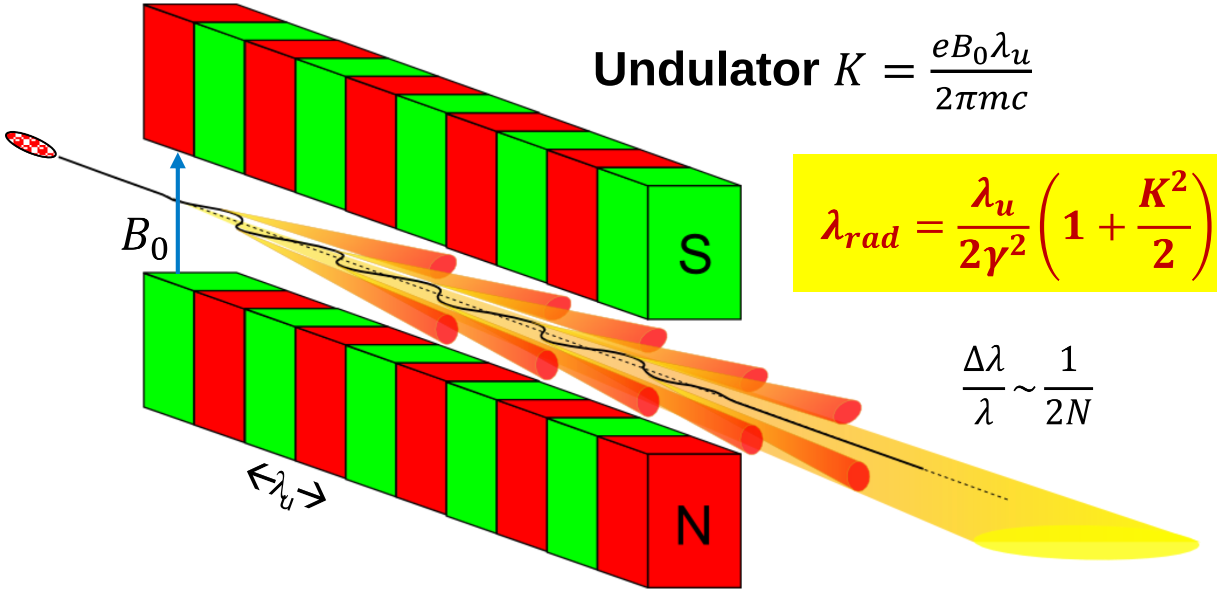

Undulator $K = \frac{eB_0\lambda_u}{2\pi mc}$

$$\lambda_{rad} = \frac{\lambda_u}{2\gamma^2}\left(1 + \frac{K^2}{2}\right)$$

$$\frac{\Delta\lambda}{\lambda} \sim \frac{1}{2N}$$

APPLE- II Undulator*

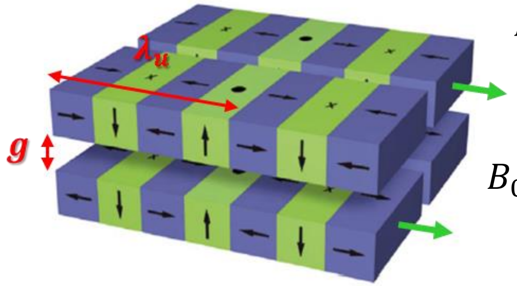

$$K = 0.934 \cdot B_0[T] \cdot \lambda_u[cm]$$

$$B_0 = 1.54e^{\left(-4.46\frac{g}{\lambda_u}+0.43\left(\frac{g}{\lambda_u}\right)^2\right)}$$

*Conceptual Design Report ST/F-TN-07/12, Fermi@Elettra, 2007

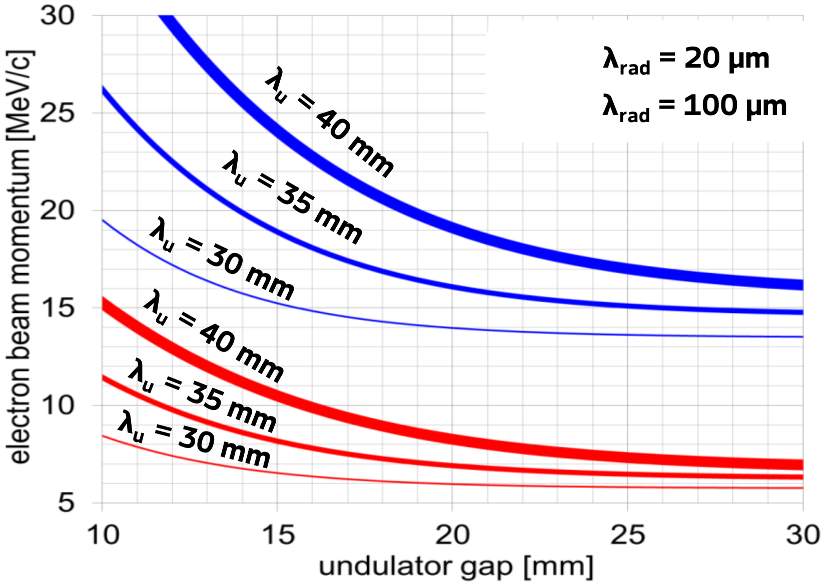

Basic Types of THz Free-Electron Lasers (FELs)

E-beam + THz undulator

THz FEL Type	Operation Principle	Pulse Structure	Advantages	Limitations / Challenges
Oscillator THz FEL 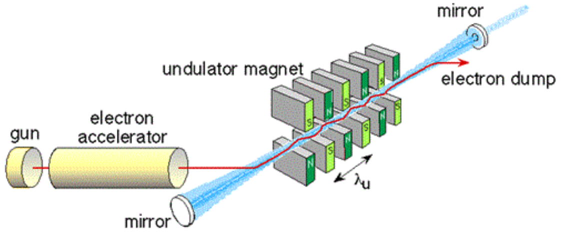	Electron beam passes through an undulator inside a resonator with optical mirrors	Continuous wave (CW) or long pulse trains	• High spectral purity • Tunable • Stable output	• Requires precise mirror alignment • Limited peak power
Superradiant THz FEL $l_b < \lambda_{rad}$ 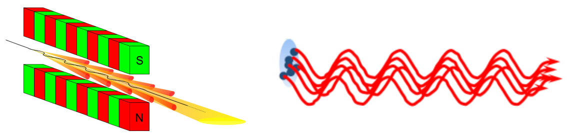	Coherent THz emission from ultrashort electron bunches in a single pass	Intense short ($l_b < \lambda_{rad}$) pulses	• Simple setup • Intense bursts possible • Tunable	• Less control over wavelength & pulse shape • Bunch compression • Slippage
Single-Pass THz FEL 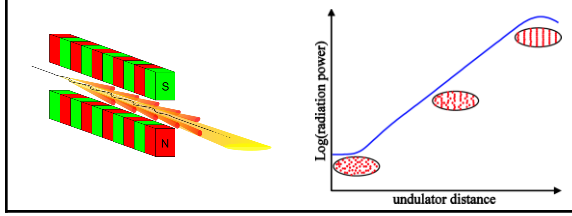	Beam passes once through the undulator; radiation is amplified without feedback	Intense "long" ($l_b > \lambda_{rad}$) high charge pulses	• High peak power • Ultrafast pulses • Tunable	• Complex beam control / matching • No spectral narrowing • Slippage

Case Studies at PITZ

Single-pass high-gain THz FEL at Photo Injector test facility at DESY in Zeuthen (PITZ)

THz@PITZ developments for pump-probe at the EuXFEL

Case Studies: PITZ-like accelerator can enable high-power, tunable, synchronized THz radiation

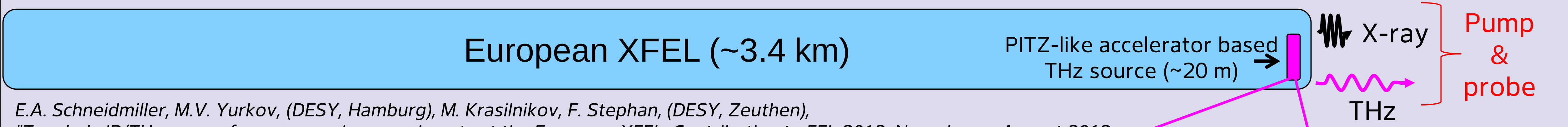

E.A. Schneidmiller, M.V. Yurkov, (DESY, Hamburg), M. Krasilnikov, F. Stephan, (DESY, Zeuthen),
"Tunabale IR/THz source for pump probe experiments at the European XFEL, Contribution to FEL 2012, Nara, Japan, August 2012

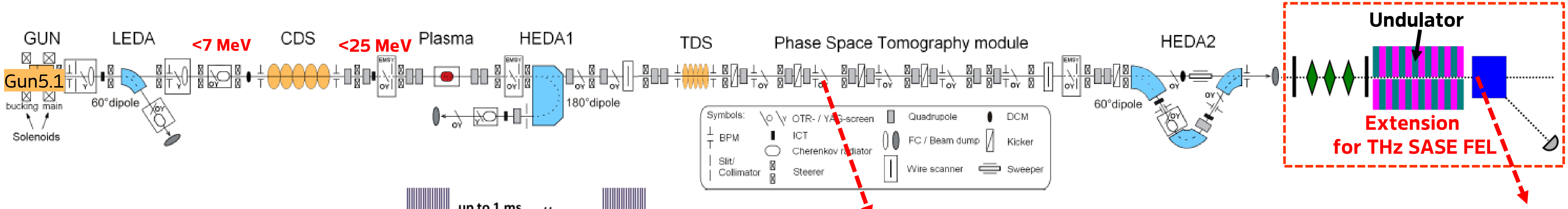

Coherent Transition Radiation (CTR) for $\lambda_{rad} \geq$ 100 µm (f ≤ 3 THz)

THz Self Amplified Spontaneous Emission (SASE) FEL for $\lambda_{rad} \leq$ 100 µm (f ≥ 3 THz)

PITZ Highlights:

- **Identical pulse train** structure as XFEL
- High **charge** feasibility (up to 6 nC), high QE photocathodes
- Advanced photocathode laser **shaping**

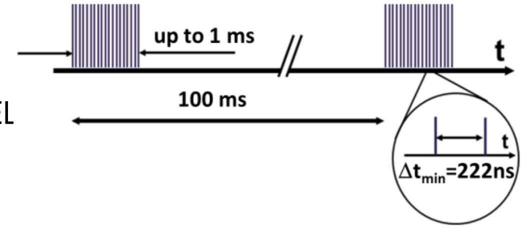

Coherent Transition Radiation (CTR)

First experience on THz CTR at PITZ (2018)

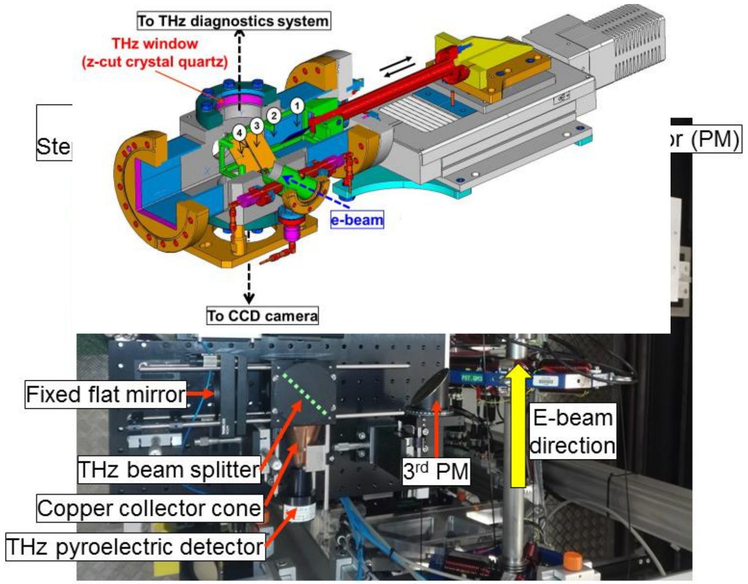

Measured (TDS) electron beam temporal profiles

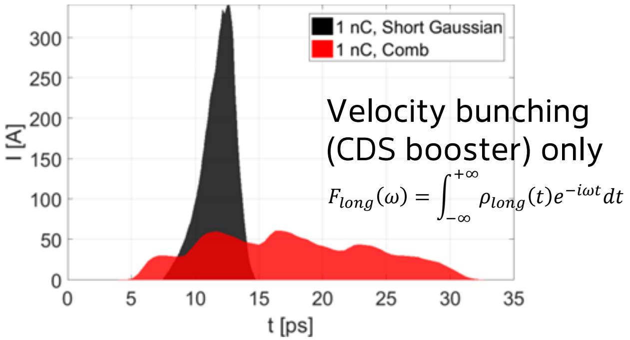

Measurements of pulse energy (THz pyroelectric detector)

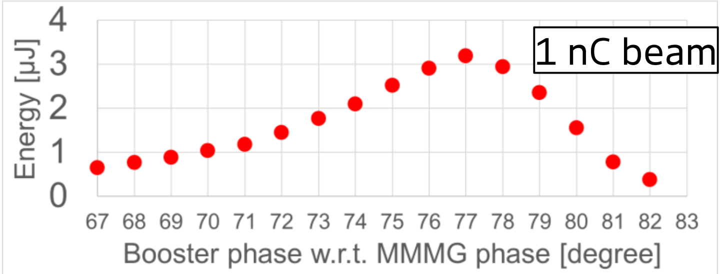

Measurements of spectra distributions (Michelson interferometer)

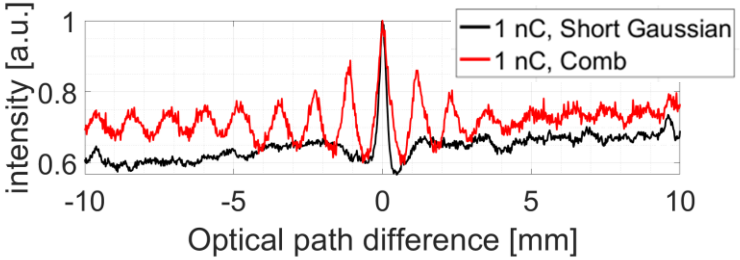

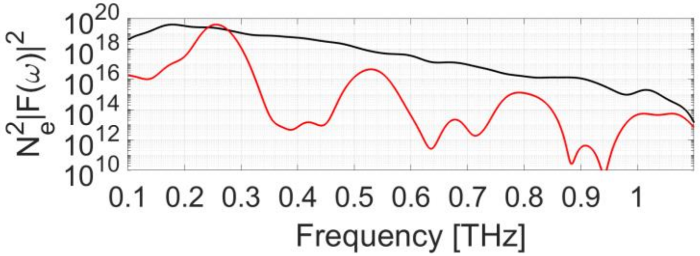

Measurements of CTR transverse profile and polarization (THz cam.)

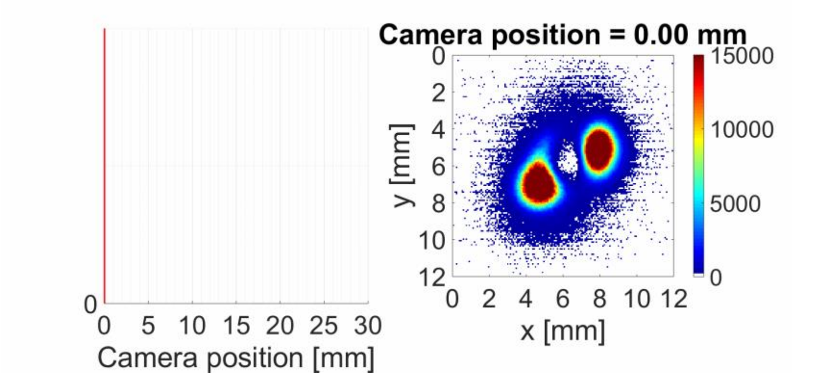

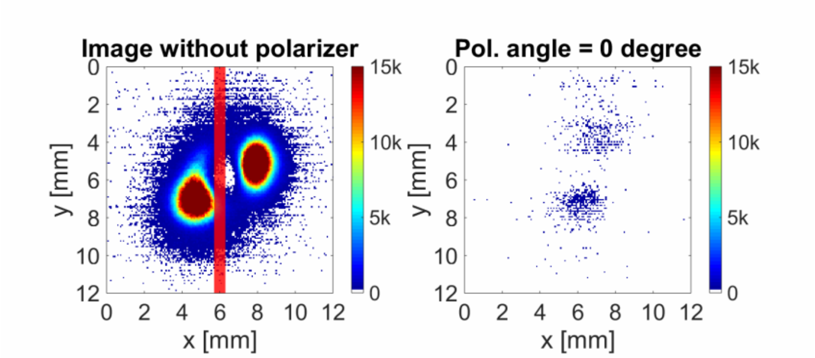

Single-pass high-gain THz FEL

Preliminary considerations

SASE FEL simulations (λ_{rad} = 100 µm) from model electron beams

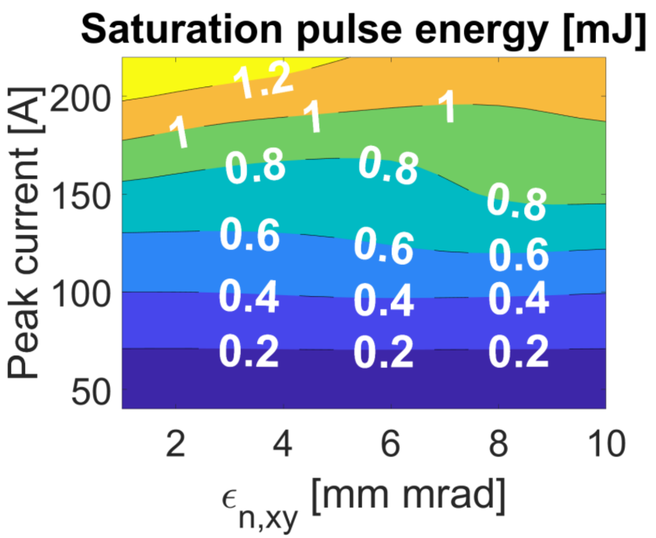

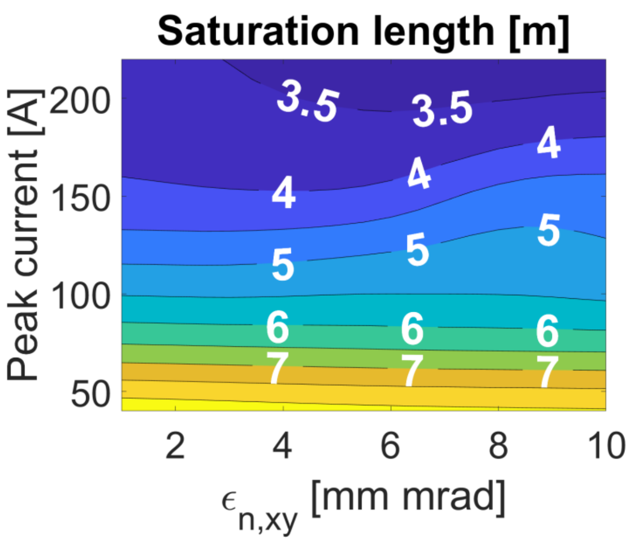

Peak current:	**50 to 200 A**
Emittance:	**1 to 10 mm mrad**

⇒

Sat. pulse energy:	**0.1 – 1.2 mJ**
Sat. length:	**3.5 – 8 m**

Properties of the APPLE-II undulator used in simulations

Property	Detail
Undulator type	Helical
K-value	1.82
Period length & total length	40 mm & 7 m (175 periods)

FEL properties from Start-to-End (S2E) simulations

Property	Detail
Central wavelength	106.4 µm
Saturation length	2.94 m
Pulse energy at saturation & U.exit	0.78 mJ & **2.51 mJ**
Peak power at saturation & U.exit	95 MW & 188.7 MW
Radiation pulse duration	18 ps (FWHM)
Spectral width	10 µm (9.4%)

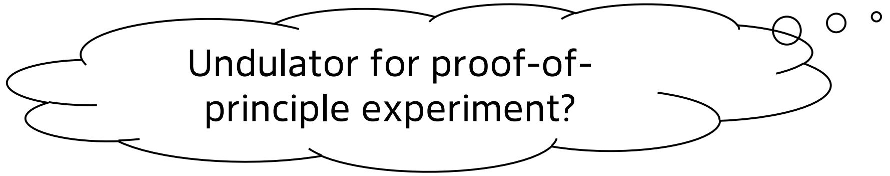

Proof-of-principle experiment on THz FEL at PITZ

Using LCLS-I undulators (available on loan from SLAC)

Some Properties of the LCLS-I undulator

Properties	Details
Type	**planar hybrid** (NdFeB)
K-value	3.585 (3.49)
Support diameter / length	30 cm / 3.4 m
Vacuum chamber size	**11 mm x 5 mm**
Period length	30 mm
Periods / a module	113 periods

Reference: LCLS conceptual design report, SLAC-0593, 2002.

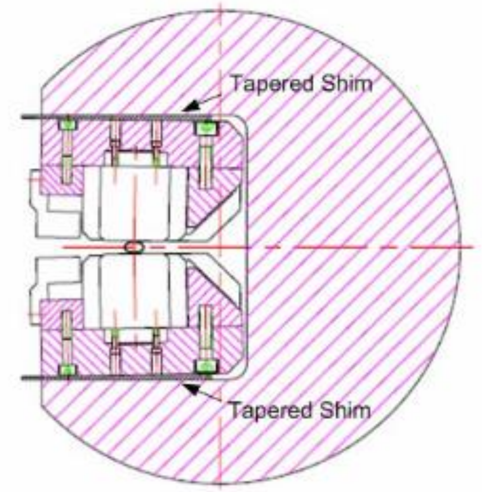

λ_{rad}~100μm → <Pz>~**17MeV/c**

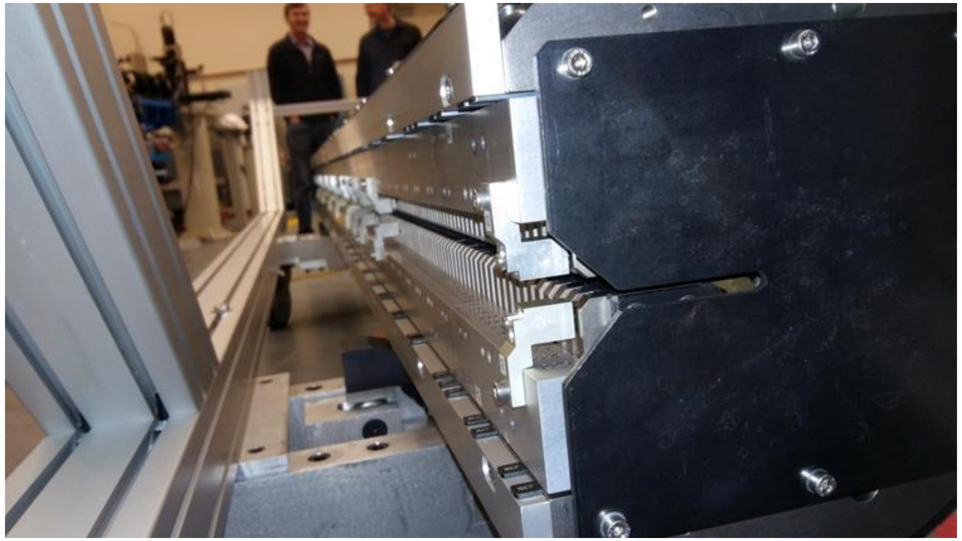

Main challenges:

- Space charge effect
- Strong undulator (vertical) focusing + horizontal gradient
- FEL parameter is not very small
- Waveguide effect
- Wakefields: geometric and conductive wall effects

LCLS-I Undulator: Magnetic Field Analysis and Modeling

LCLS-I undulator module L143-112000-26 (on-loan from SLAC) re-measured at DESY in Hamburg

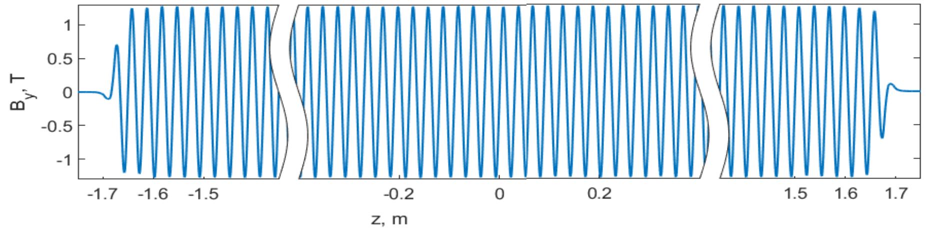

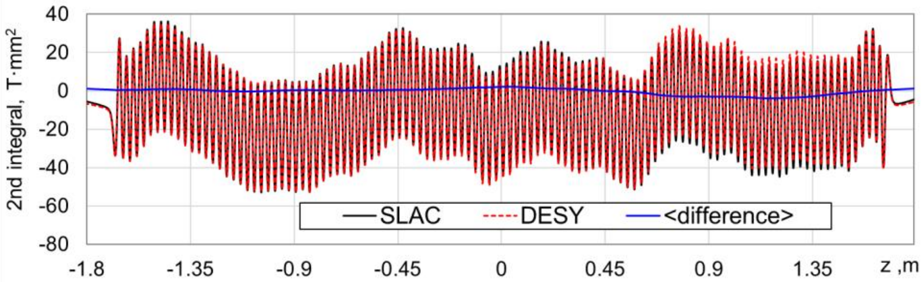

$$\chi(x,y,z) = -\frac{\cosh[k_x(x_0+x)]}{\cosh[k_x x_0]} \cdot \sum_{n=1}^{N_h \cdot N_U} \{a_n \cos(k_{zn} z) + b_n \sin(k_{zn} z)\} \cdot \frac{\sinh(k_{yn} y)}{k_{yn}}$$

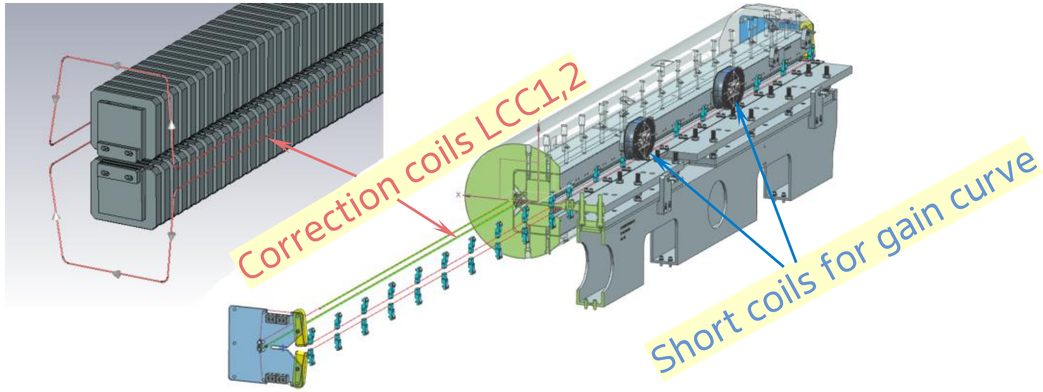

Horizontal Gradient Modeling

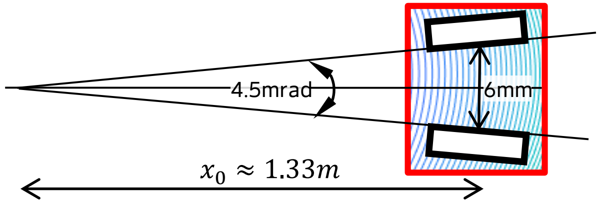

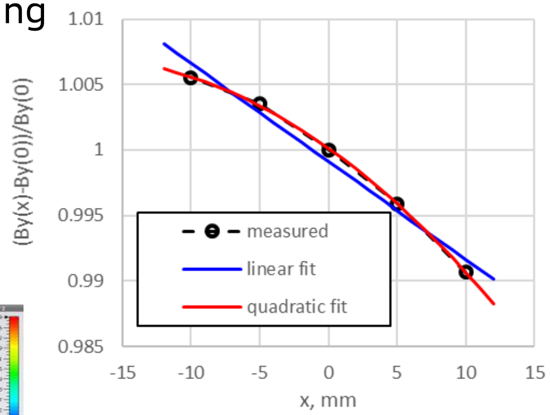

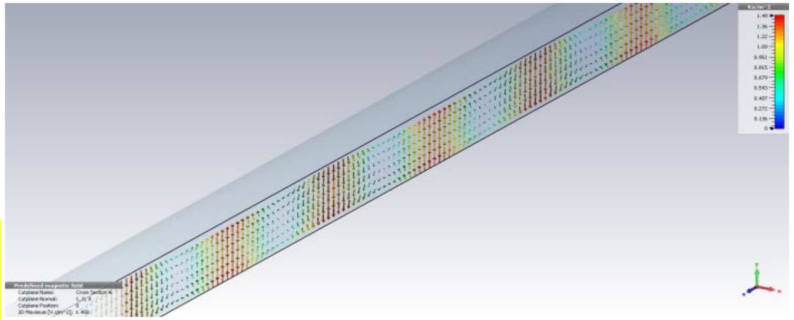

Reference particle trajectories in the undulator with horizontal gradient

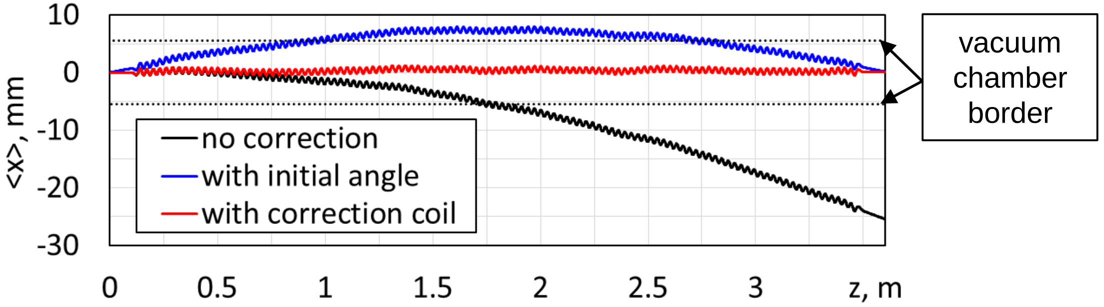

PITZ beamline extension

Design and technical Implementation

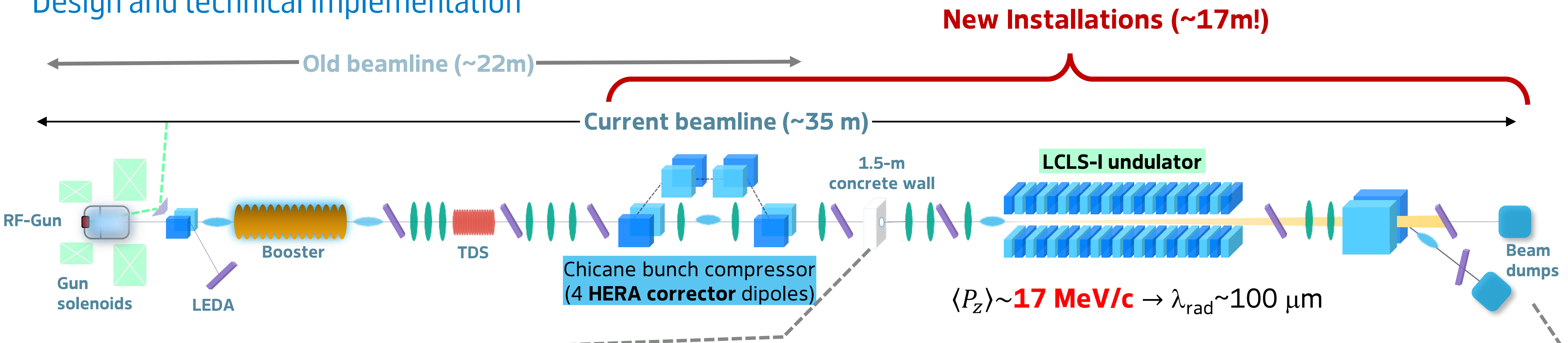

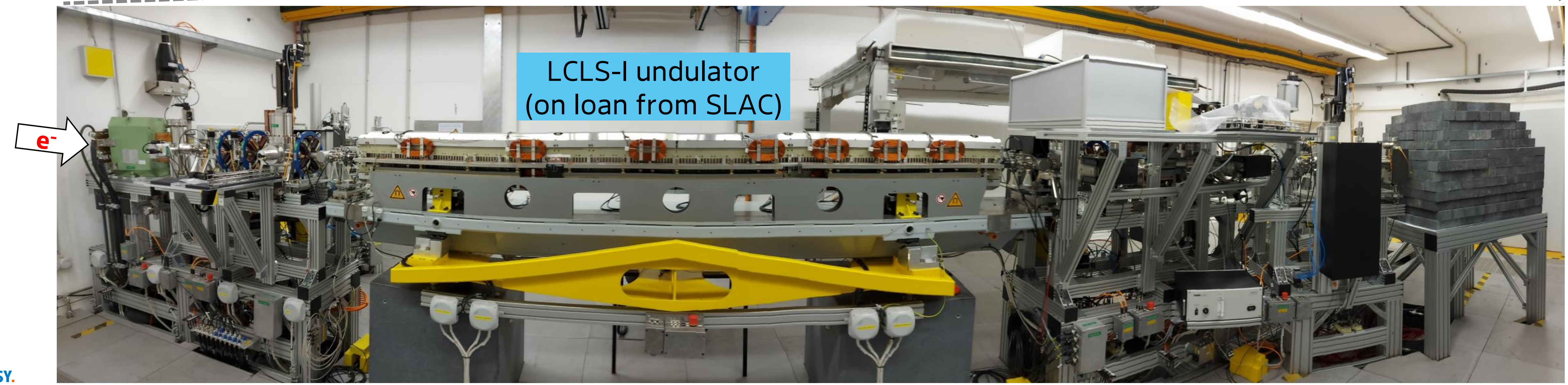

Single-pass high-gain THz FEL at PITZ: beam transport

Quasi-round space charge dominated (2nC, 17MeV/c) beam transport over ~30m

- In total, **four quadrupole triplets** are used to focus and match the beam from the booster to the undulator
- With the **first three triplets**, the beam is focused equally in both transverse planes ($\sigma_x \sim \sigma_y$) → quasi-round beam transport
- The **4th** quadrupole triplet is used for the beam (strongly asymmetric, $\sigma_x \gg \sigma_y$; $\beta_x \gg \beta_y$) matching into the LCLS-I undulator
- The beam **emittance ($\varepsilon_{n,x}$, $\varepsilon_{n,y}$)** oscillates under the space charge forces and the focusing forces from the quadrupoles

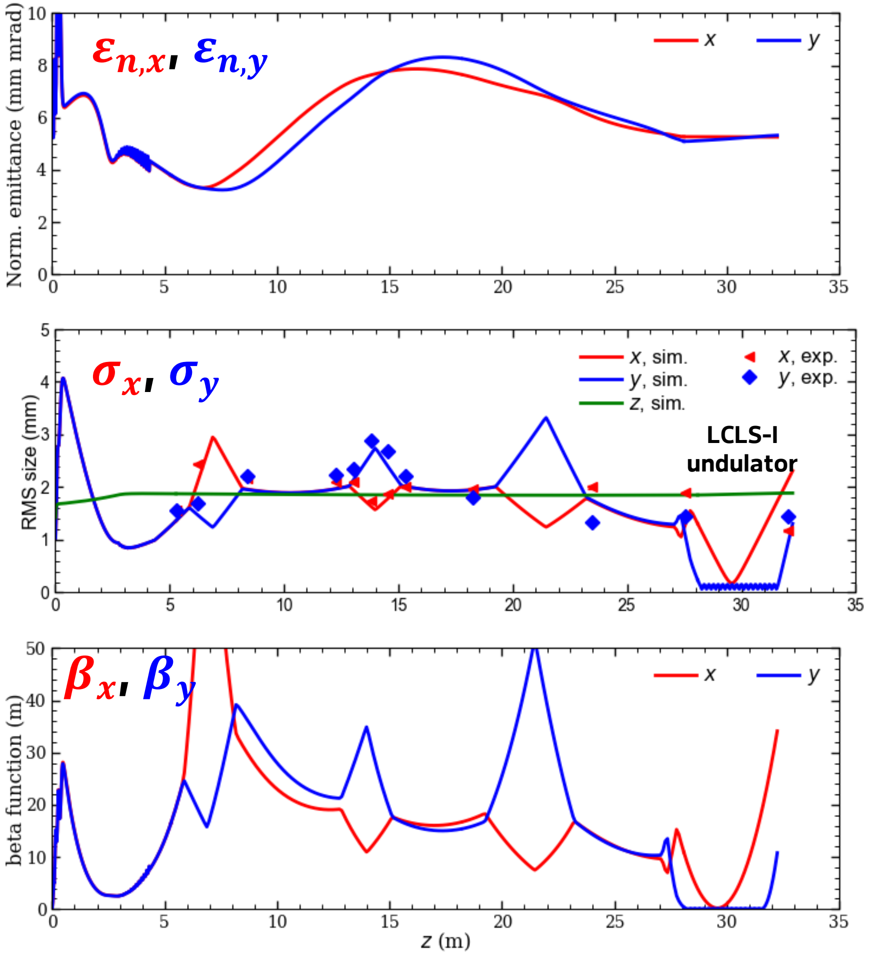

Courtesy X-K. Li

- Lines from (**Astra and Ocelot**) simulations
- Markers are from measurements

DESY.

Single-pass high-gain THz FEL at PITZ: beam matching

Main challenge: electron beam matching (2nC, 17MeV/c) for lasing

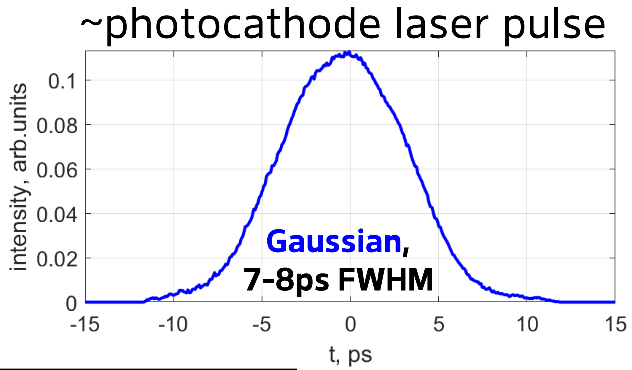

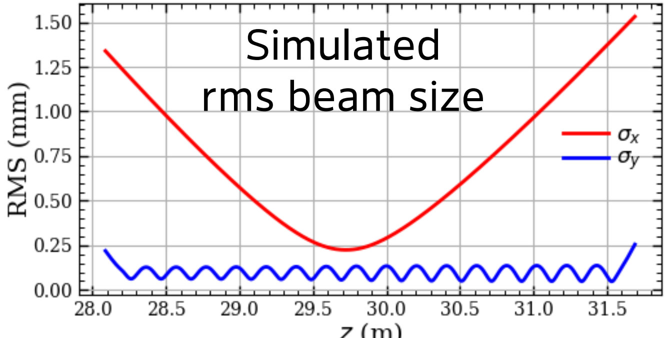

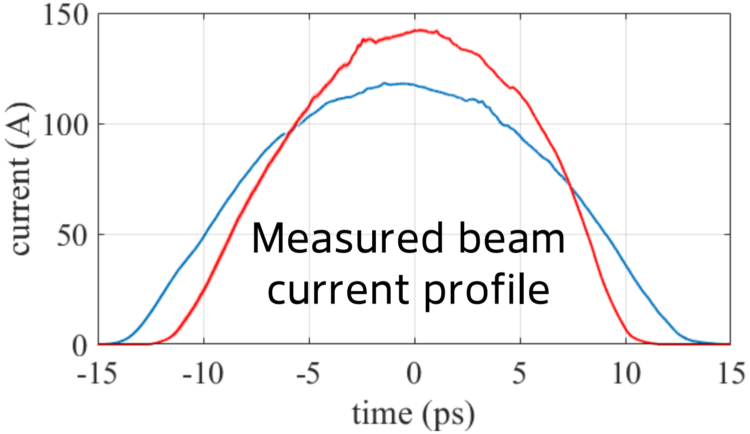

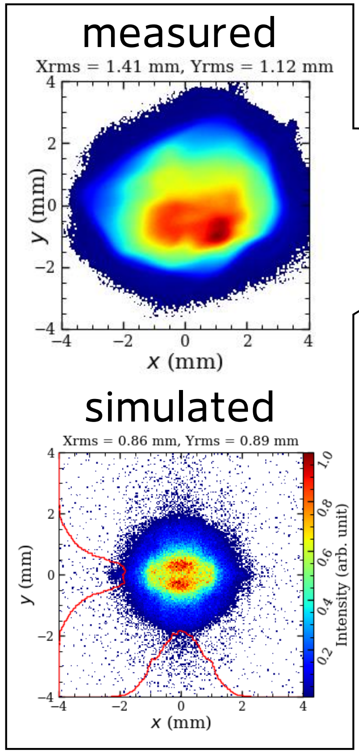

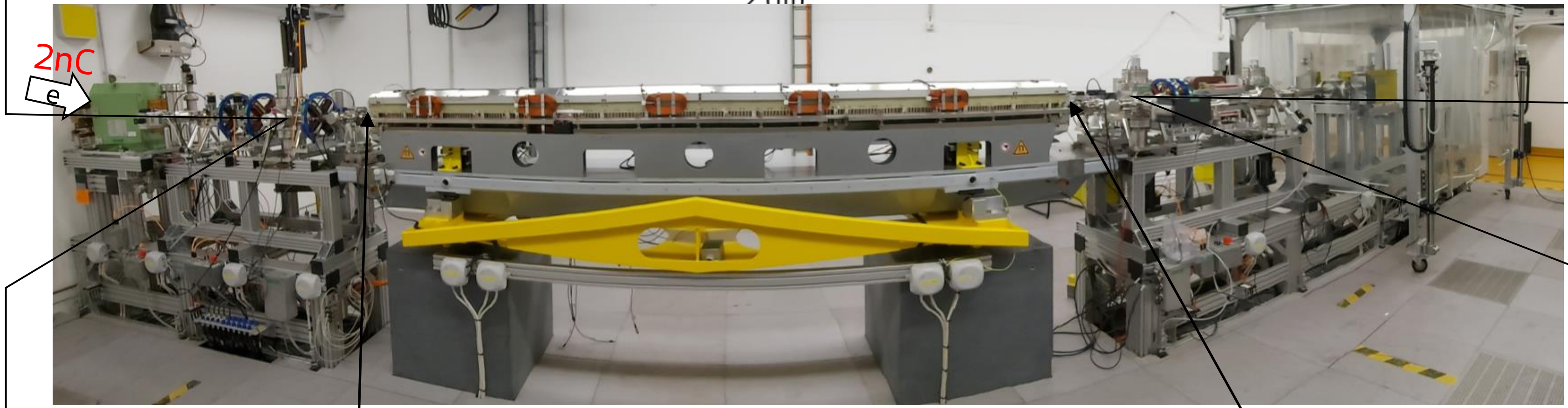

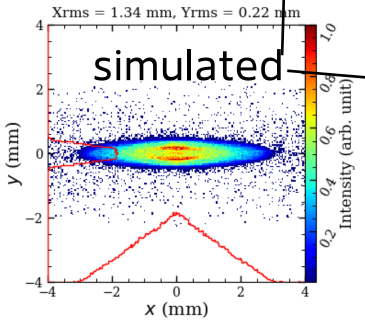

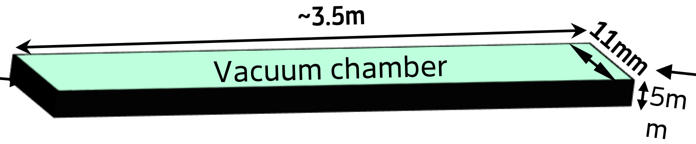

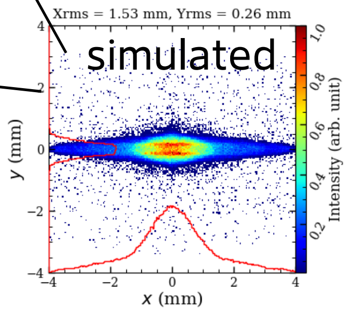

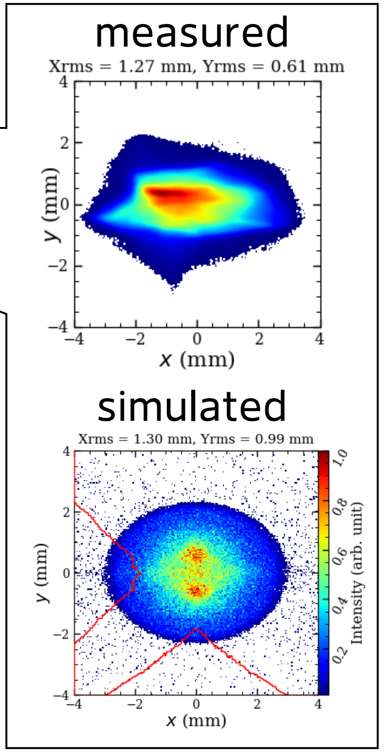

X. Li et al., "Matching of a Space-Charge Dominated Beam into the Undulator of the THz SASE FEL at PITZ", in Proc. 12th Int. Particle Accelerator Conf. (IPAC'21), Campinas, Brazil, May 2021, pp. 3244-3247.

THz at PITZ Characterization

THz Diagnostics

Simplified layout of the gain curve measurement setup

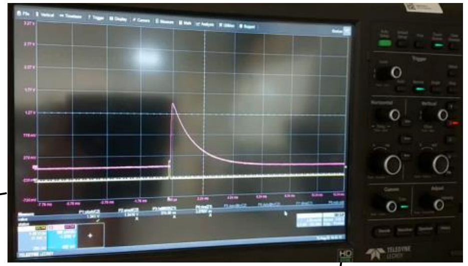

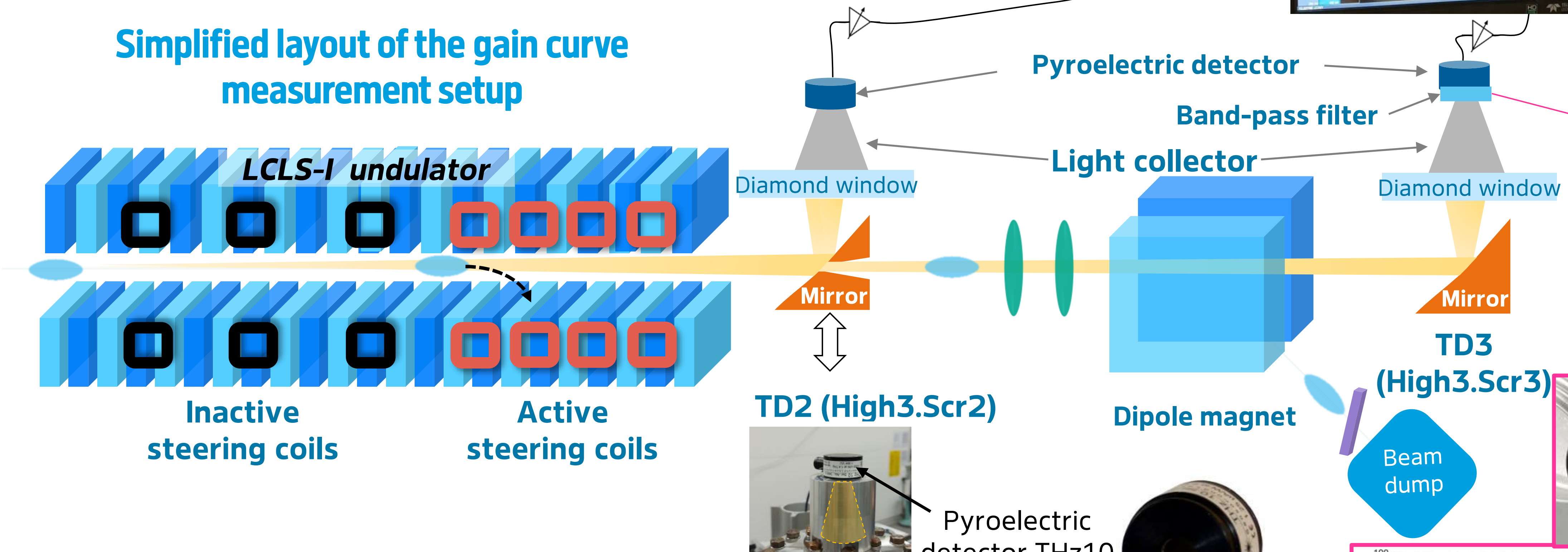

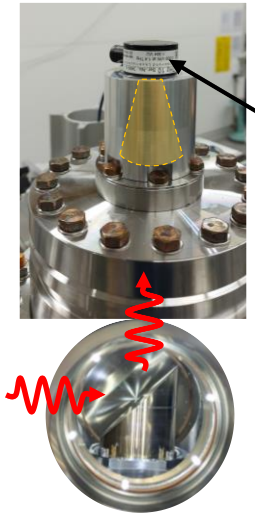

Pyroelectric detector THz10
SLT Sensor- und Lasertechnik GmbH

BPF3.0-24
λ_0~102μm
$\delta\lambda$~12μm

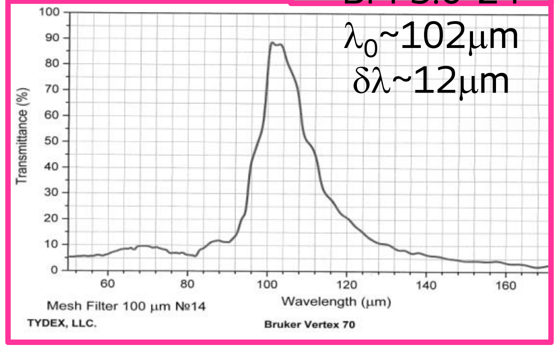

	High3.Scr2	High3.Scr3
Estimated transmission	49%	63%

DESY.

Gain Curves at TD3 with BPF

In-vacuum mirror without hole + 3THz Band-pass filter

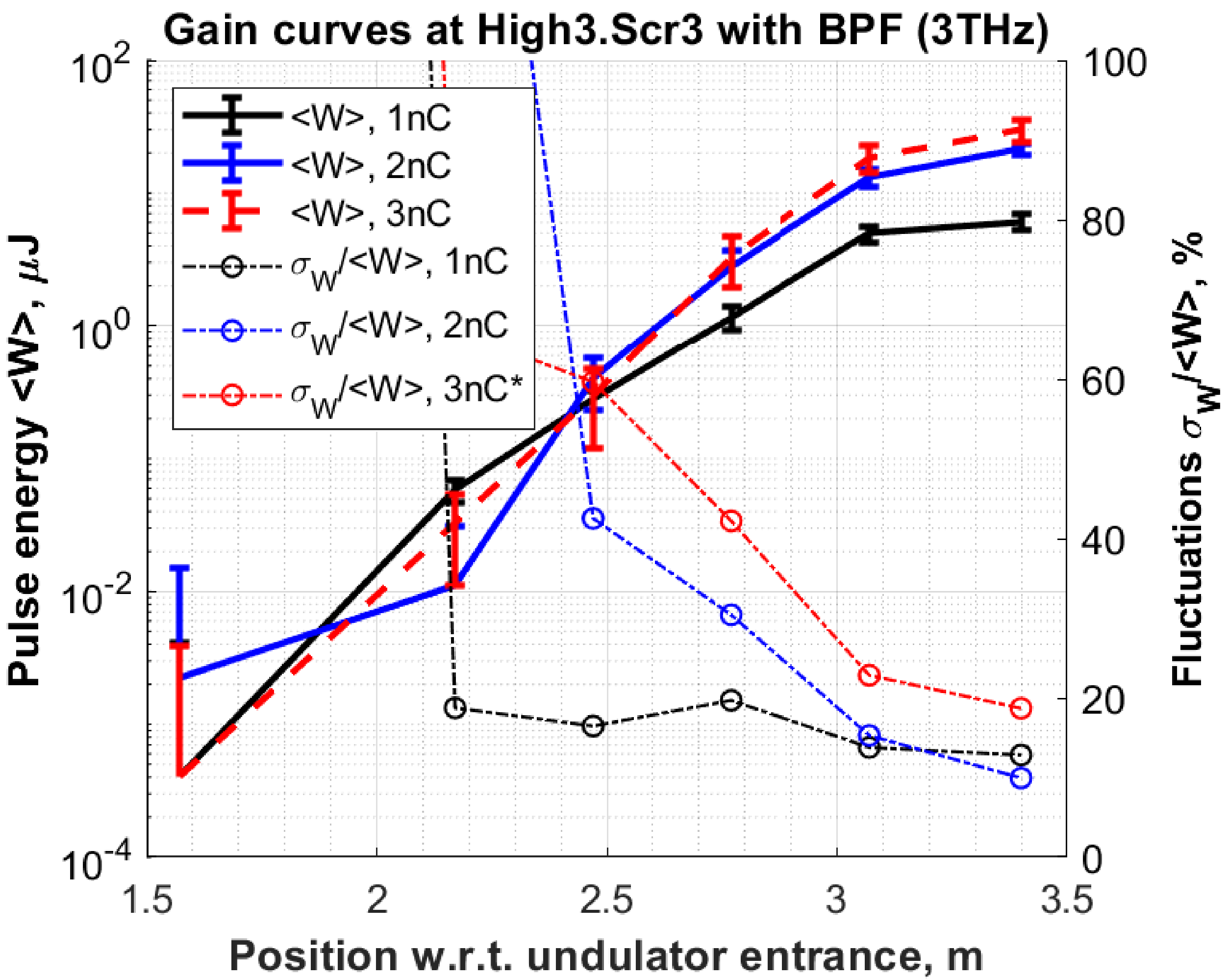

Optimization progress
<pulse energy> (fluctuations)
TD2 vs TD3


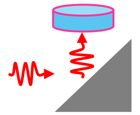

Bunch charge	1st lasing, no BPF	Tuning, BPF
1nC	0.36 uJ (32%)	6.12uJ (13%)
2nC	0.55uJ (52%)	21.44uJ (10%)
3nC*	2.26uJ (78%)	29.67uJ (19%)

* Not fully optimized

First Seeding Experiments

SASE vs. seeded THz FEL with modulated photocathode pulse (preliminary results)

- Gain Curves at TD3 (THz mirror w/o hole) with BPF
- THz FEL Seeding experiments
  (**2nC** e-beam with modulated photocathode laser pulse):
  <W>→ **33μJ** vs **21μJ** from SASE

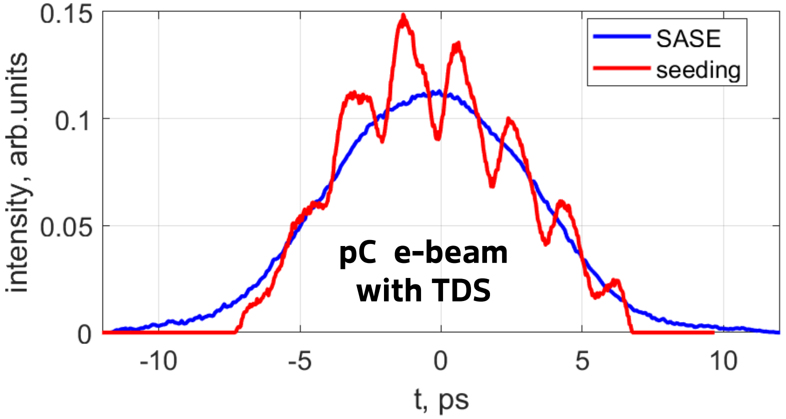

P_z-distributions of e-beam (2nC) after gun (LEDA)

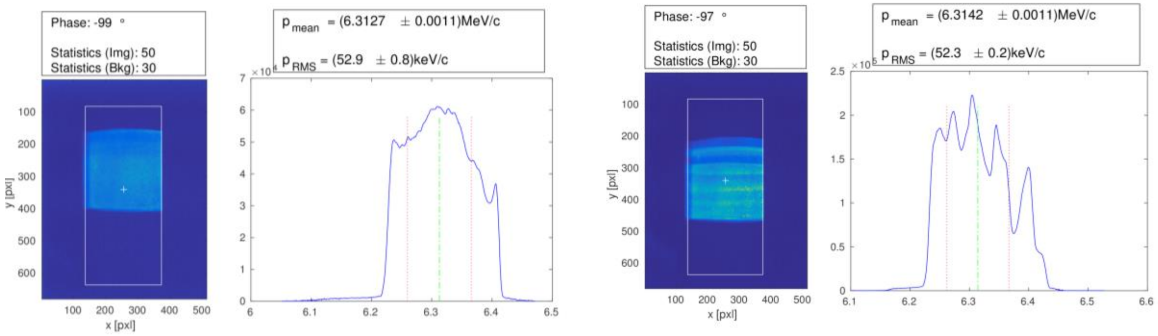

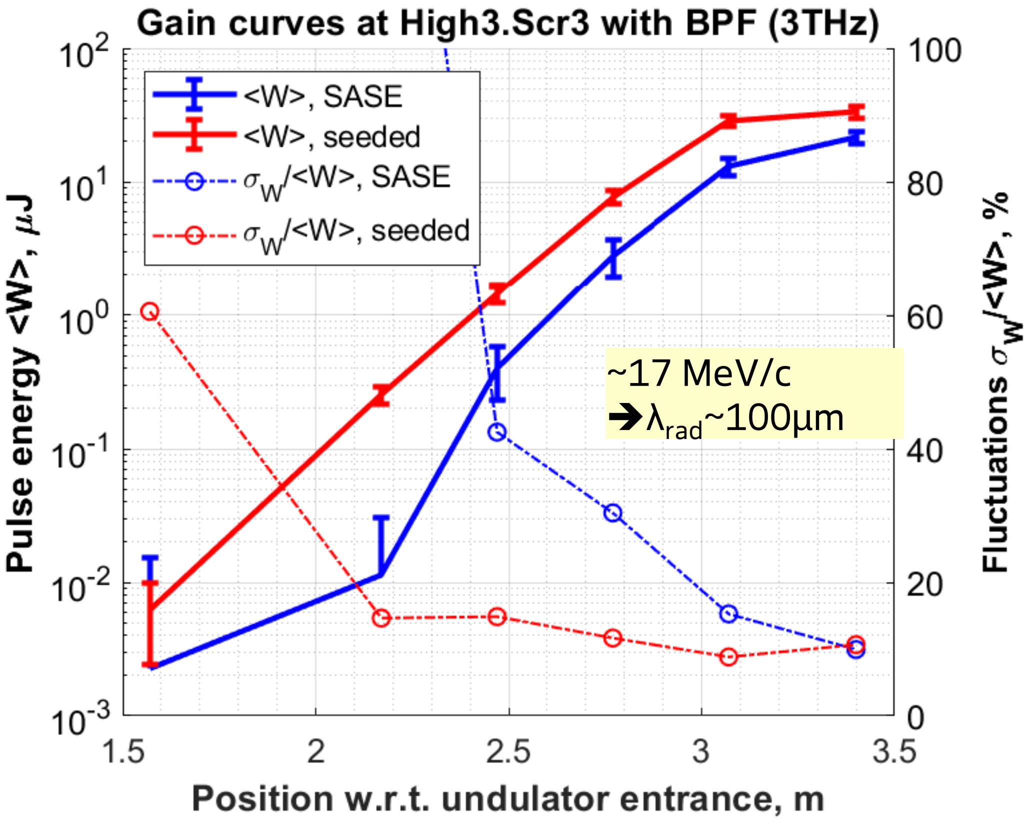

Seeded THz FEL gain curve:
- Higher energies + earlier start
- Better stability

M. Krasilnikov, et al., Phys. Rev. Accel. Beams., 28(3):030701, 2025

THz FEL at PITZ: TD2 vs TD3

THz generation and transport

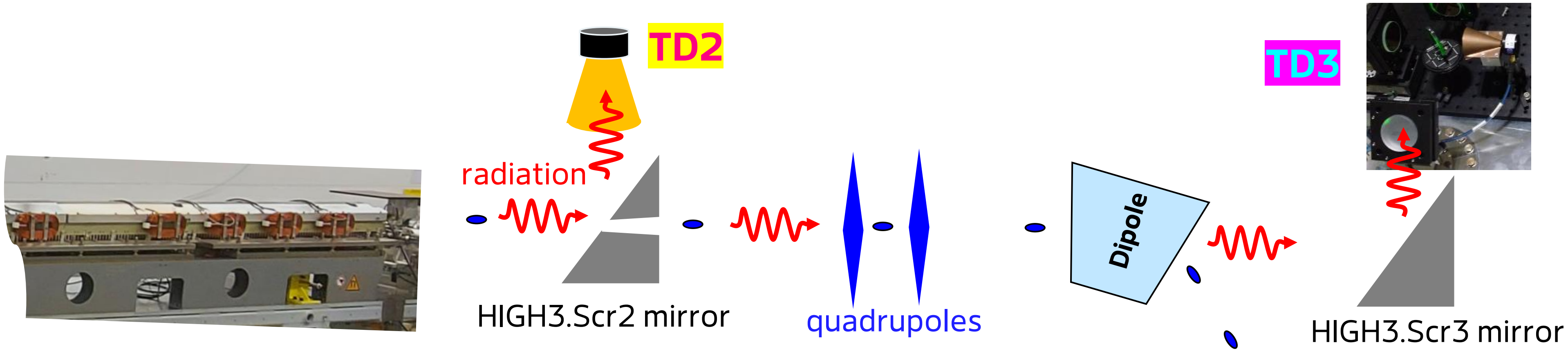

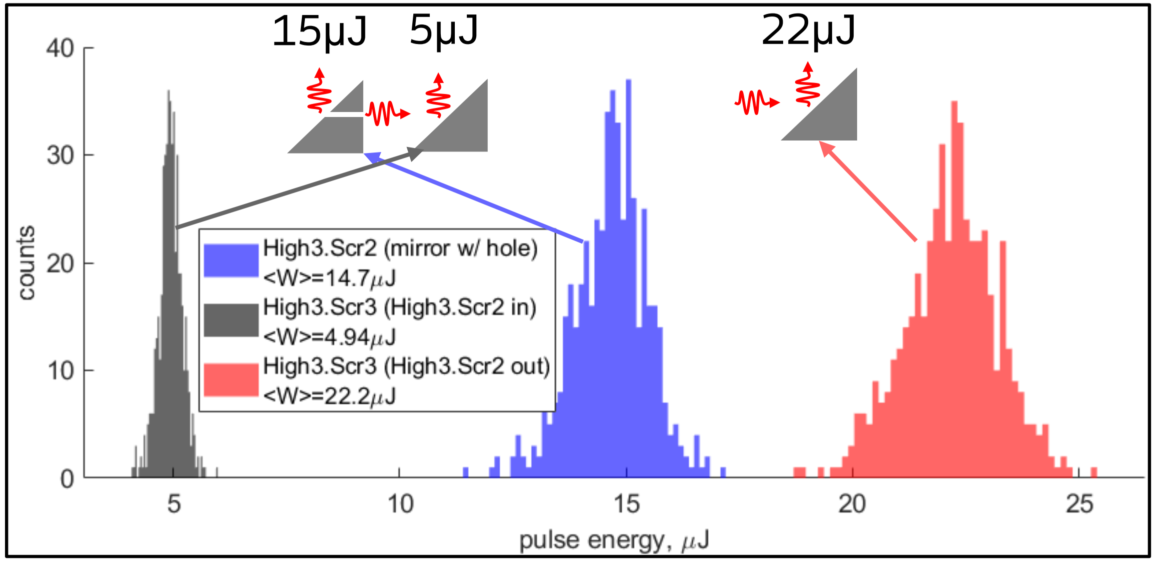

DESY.

Electron beam in dispersive section and pyro- signals

Microbunching observation

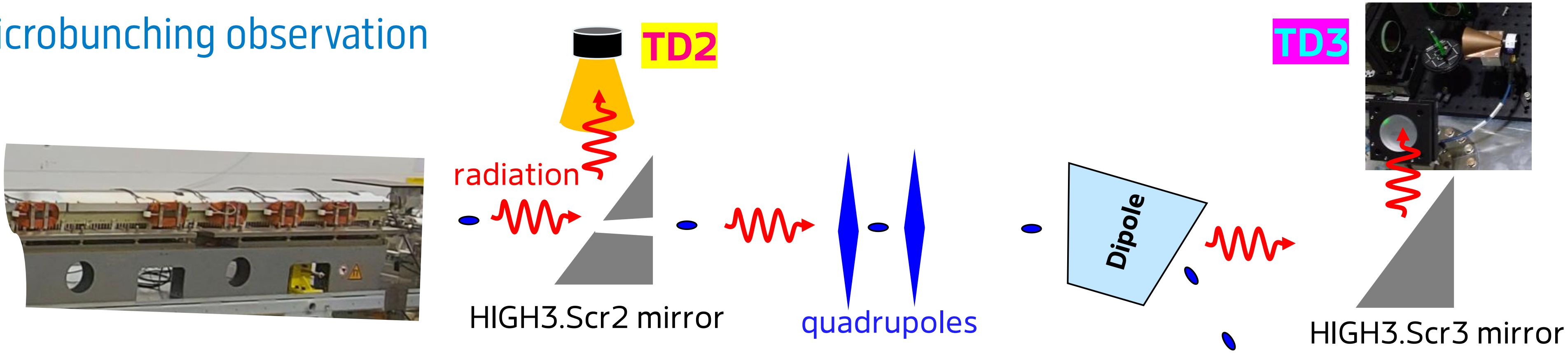

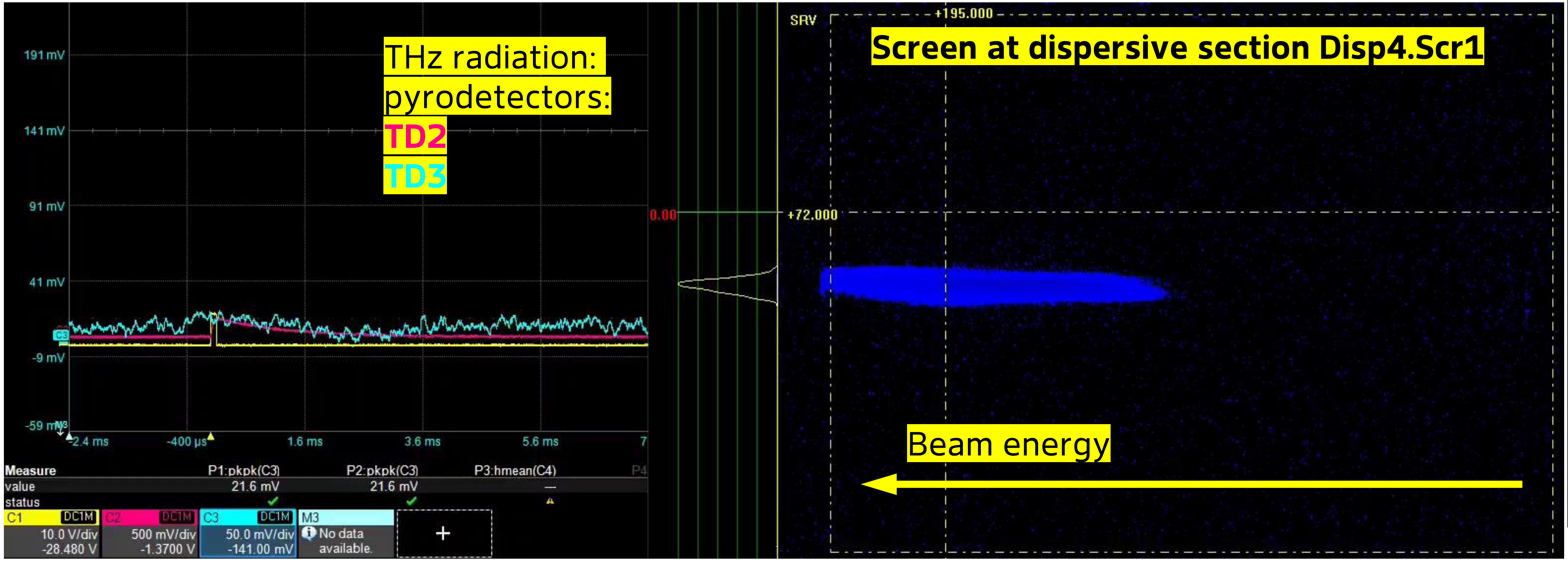

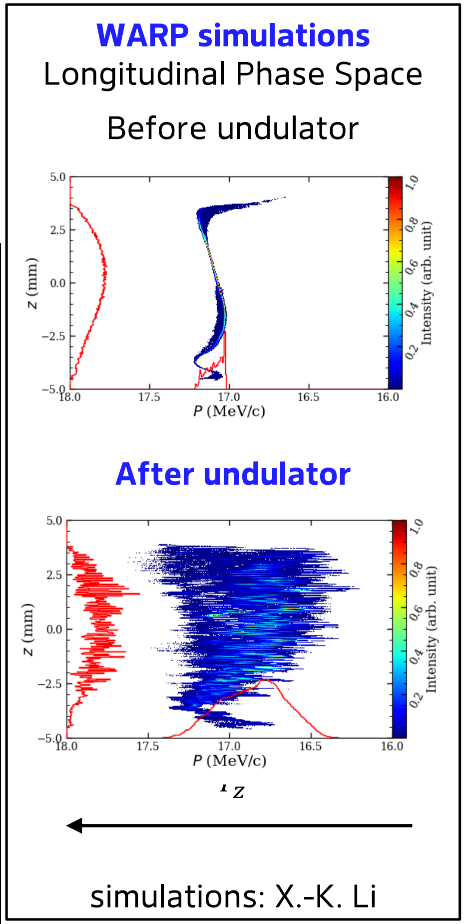

DESY.

Improving THz radiation output

Automatization of the THz FEL optimization

Bayesian optimizer (Matlab) is used to optimize the **beam trajectory** and **phase spaces** maximizing the THz output

- Two pairs of steering coils → trajectory
- Four to six quadrupole magnets → transverse phase space
- Booster phase → longitudinal phase space

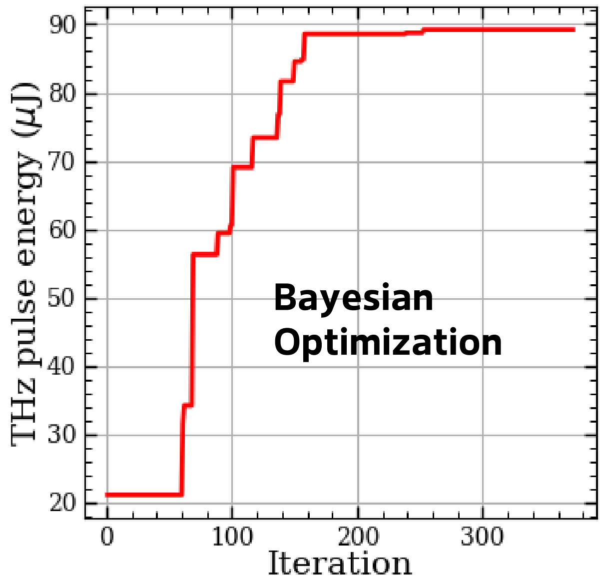

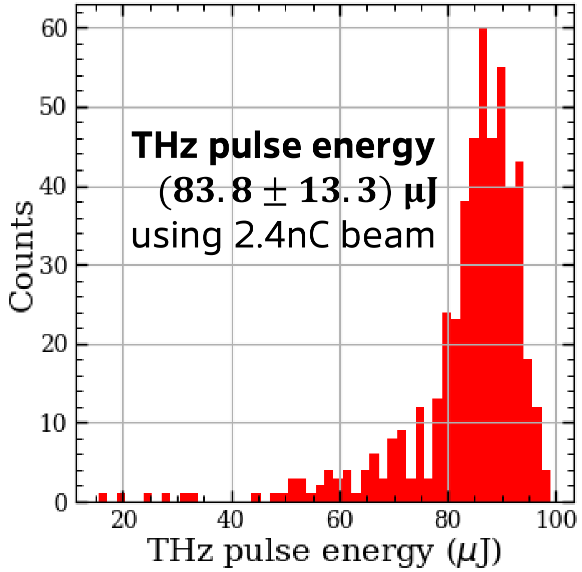

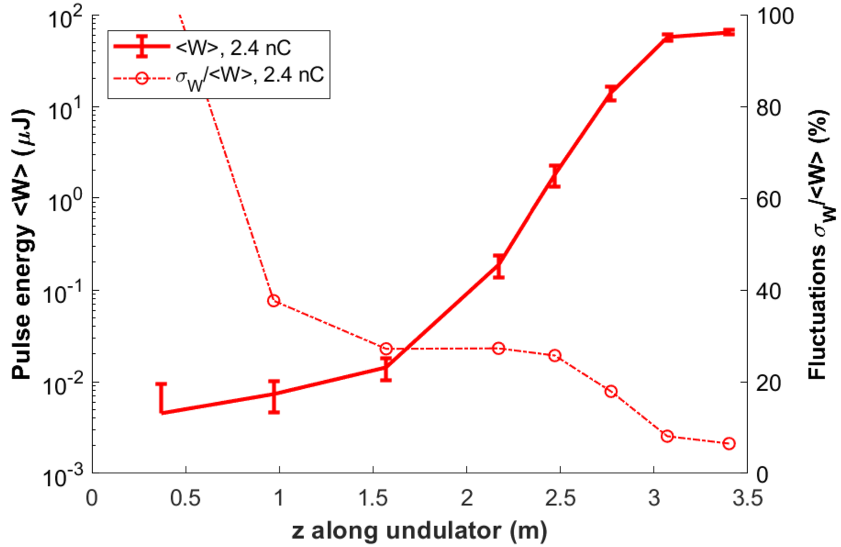

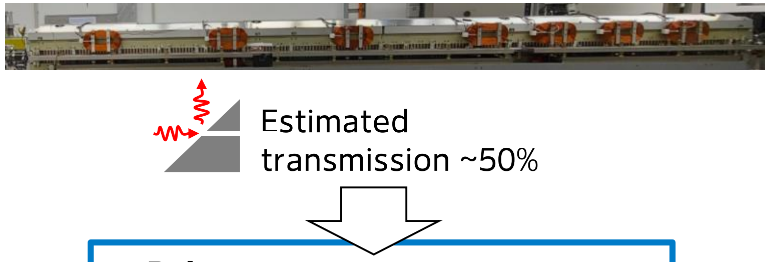

- **Pulse energy:**
  - **> 100μJ generated**
  - Energy fluctuations ~6-10%

M. Krasilnikov, et al., Phys. Rev. Accel. Beams., 28(3):030701, 2025

THz at PITZ Characterization: Spectral measurements

THz spectrum by FTIR (E. Zapolnova)

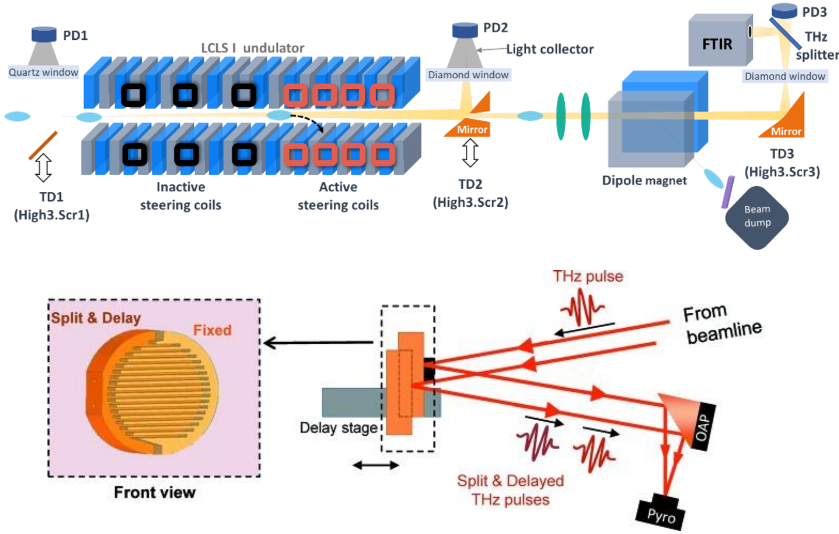

Pan, R. et al.,, "Photon diagnostics at the FLASH THz beamline," J. Synchrotron Rad., vol. 26, pp. 700-707, 2019.

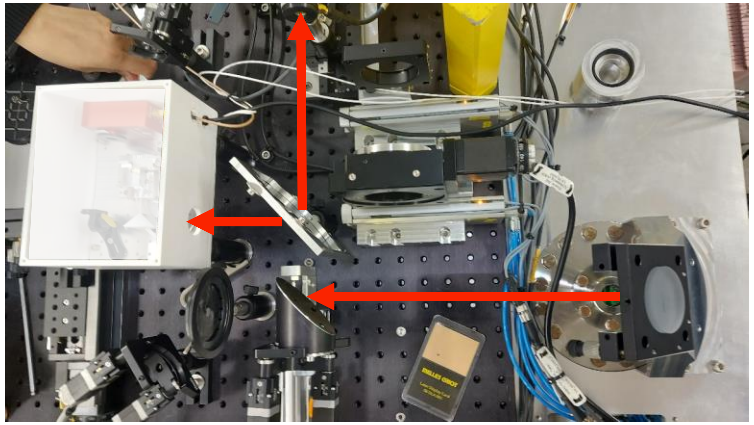

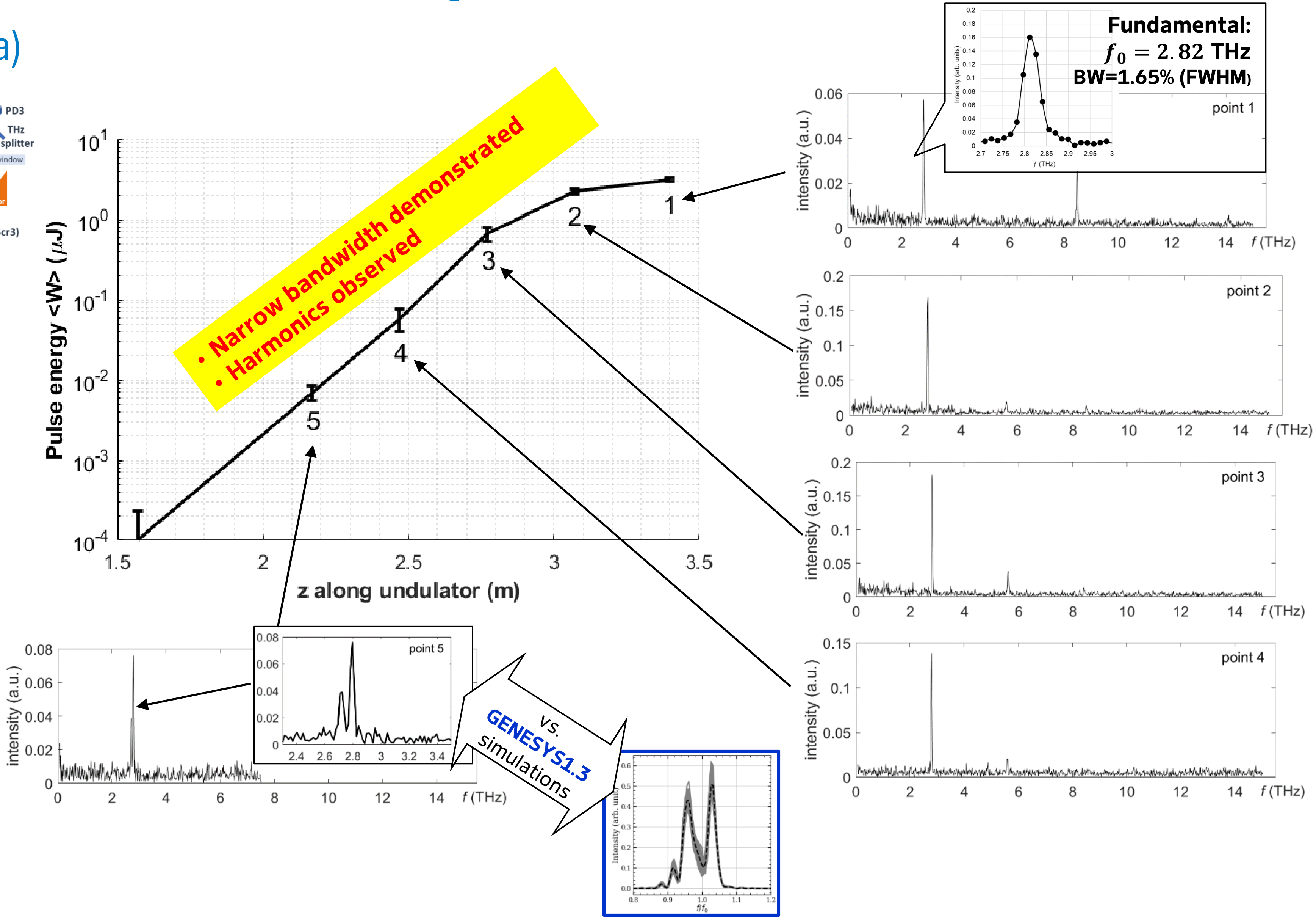

THz at PITZ Characterization: Transverse distribution

Images with THz camera (**Pyrocam IIIHR**) along gain curve

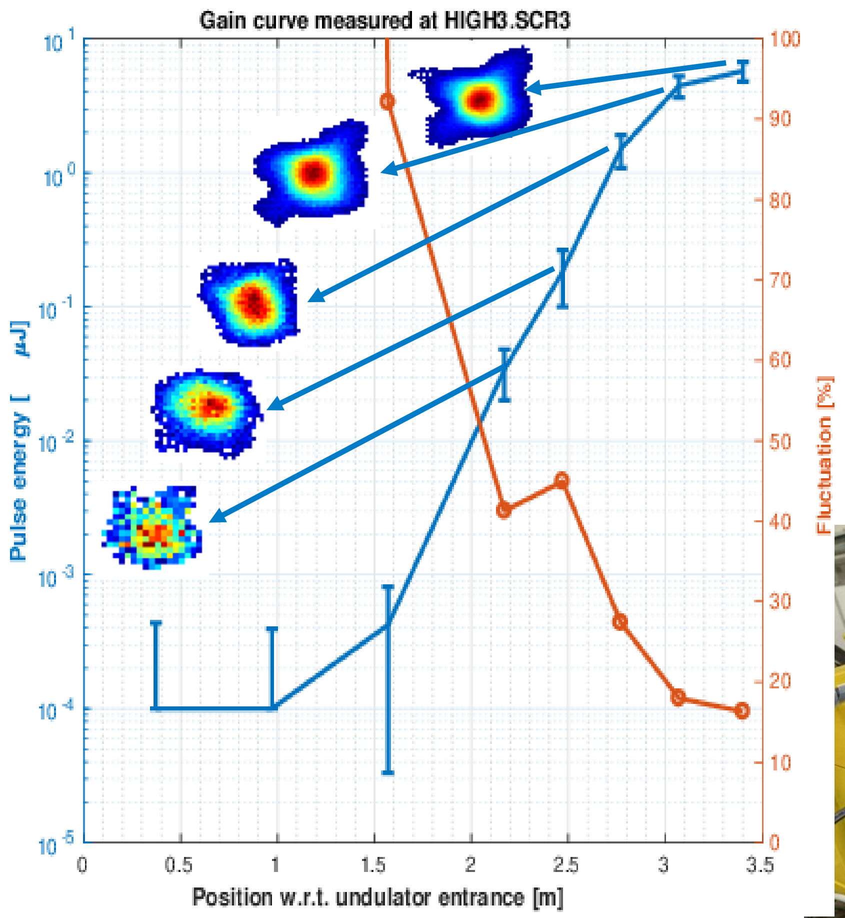

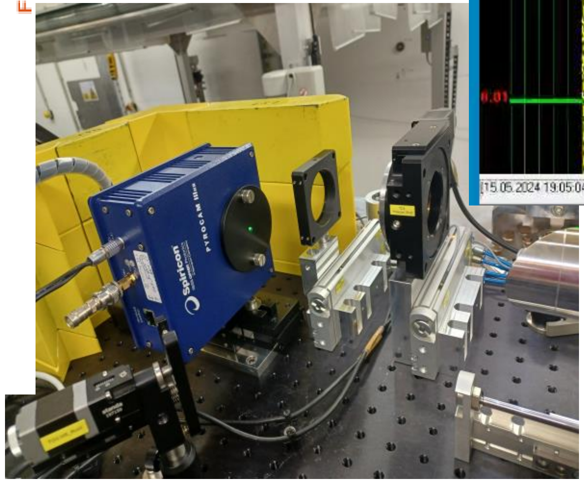

Courtesy N. Aftab

Polarizer angle scan and THz transverse profile on camera

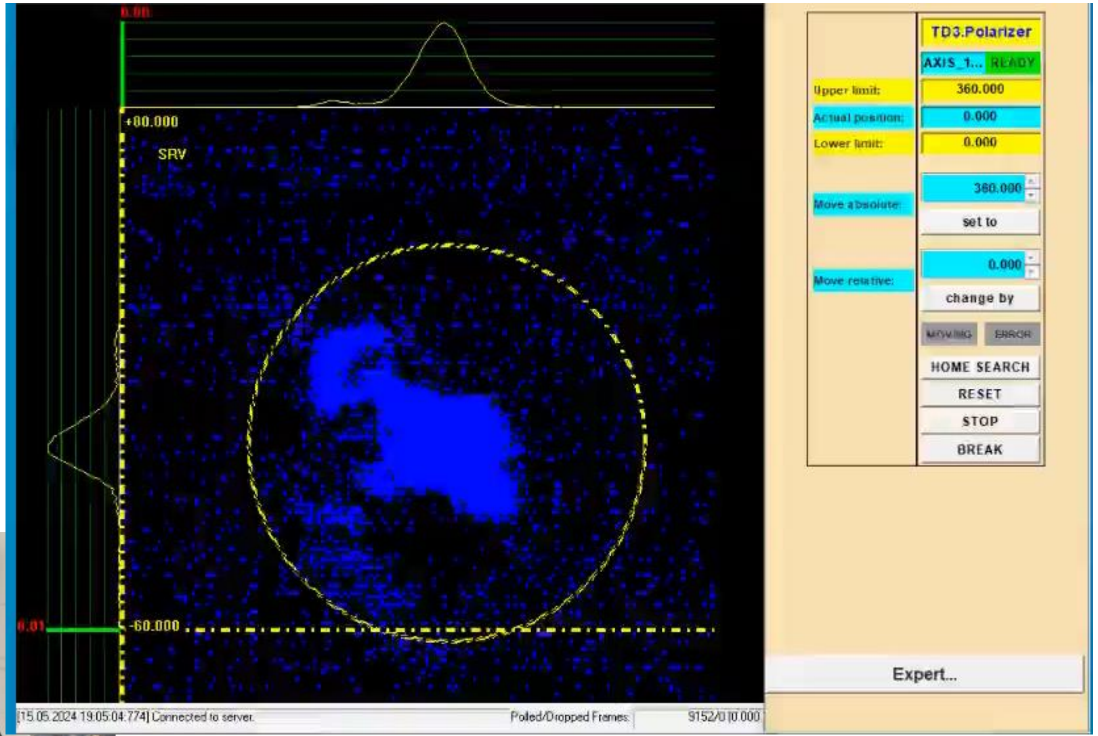

Improving alignment of optics!

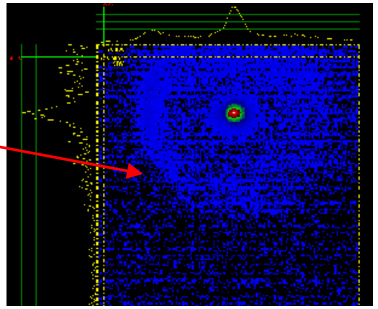

Modeling and simulations of THz FEL

Single-pass high-gain THz FEL at PITZ

Reference case: 2nC

Cross-check with linear theory of FEL amplifier with diffraction effects

e-beam

parameter	value
Energy, E_0	~17MeV
γ	34
$<\sigma_x>$	0.75mm
$<\sigma_y>$	0.2mm
$<\sigma_r>$	0.55mm
charge	2nC
I_{peak}	125A
$\varepsilon_{n,x,y}$	5 mm mrad
σ_E	~10keV (slice)

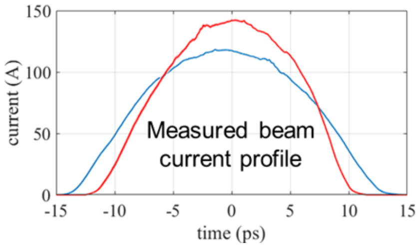

FEL radiation

parameter	value
λ_{rad}	~90µm
Q	0.429
A_{JJ}	0.745
θ_l	0.10
γ_l	12.6
Γ	$(0.237\text{m})^{-1}$

$$\lambda_{rad} = \frac{\lambda_w}{2\gamma^2}\left(1+\frac{K^2}{2}\right)$$

$$Q = \frac{K^2}{4+2K^2}$$

$$A_{JJ} = J_o(Q) - J_1(Q)$$

$$\theta_l = K/\gamma$$

$$\frac{1}{\gamma_l^2} = \frac{1}{\gamma^2} + \frac{\theta_l^2}{2}$$

$$\Gamma = \sqrt{\frac{I_{peak}A_{JJ}^2\omega^2\theta_l^2}{2I_A c^2\gamma_l^2\gamma}}$$

FEL dimensionless

Parameter		Value
Diffraction	B	~0.1
SC	$\hat{\Lambda}_p^2$	0.9
FEL	ρ	0.01
EnSpread	$\hat{\Lambda}_T^2$	0.003
Waveguide	$\Omega*$	5.3

$$B = \frac{2\Gamma\sigma_r^2\omega}{c}$$

$$\hat{\Lambda}_p^2 = \frac{4c^2}{[\theta_l\sigma_r\omega A_{JJ}]^2}$$

$$\rho = \frac{\gamma_l^2\Gamma}{\omega/c}$$

$$\hat{\Lambda}_T^2 = \frac{\sigma_E^2}{[E_o\rho]^2}$$

$$\Omega = \Gamma R_{eff}^2\omega/c$$

undulator system

parameter	value
λ_u	30mm
K	3.34 (3.47)
Vacuum chamber R_{eff}	4.2mm

$$E_x(z) \propto \exp(\Lambda \cdot z)$$

Reference: Saldin E.L., Schneidmiller E.A., Yurkov M.V. "The physics of free electron lasers" - Berlin et al.: Springer, 2000.

Reference case: 2nC

Cross-check with linear theory of FEL amplifier with diffraction effects

The gain parameter of the FEL amplifier

$$\Gamma = \sqrt{\frac{I_{peak} A_{JJ}^2 \omega^2 \theta_l^2}{2 I_A c^2 \gamma_l^2 \gamma}} = (0.237m)^{-1}$$

Parameter		Value
Diffraction	B	~0.1
SC	$\hat{\Lambda}_p^2$	0.9
FEL	ρ	0.01
EnSpread	$\hat{\Lambda}_T^2$	0.003
Waveguide	$\Omega*$	5.3

Expected power spectrum (the high gain regime at the onset of saturation)

Reference: E.L. Saldin, E.A. Schneidmiller and M.V. Yurkov, "On a theory of an FEL amplifier with circular waveguide and guiding magnetic field", Nucl. Instr. Meth. A 375, p. 241, 1996.

Eigenvalue problem →beam radiation modes

$E_x(z) \propto \exp(\Lambda \cdot z)$, Λ → field gain (ReΛ)

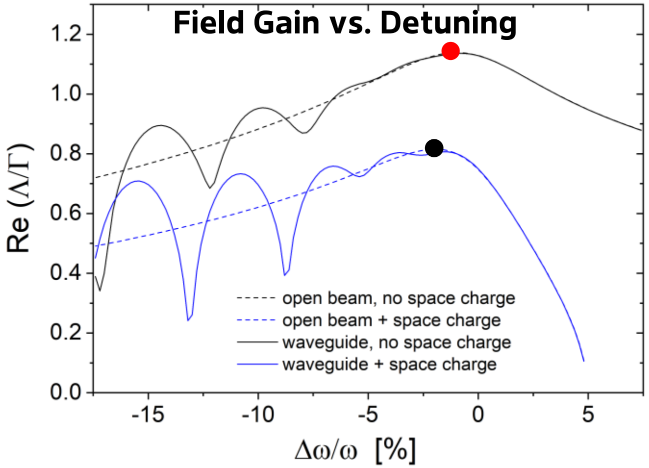

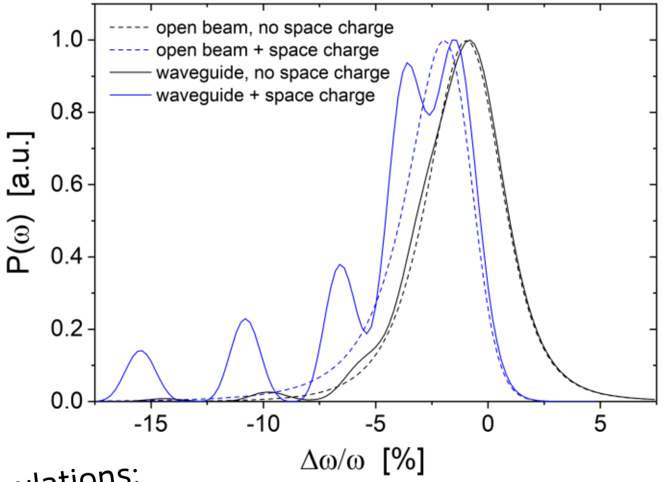

Calculations: courtesy M. Yurkov

THz FEL at PITZ 2nC: Linear theory versus measurements

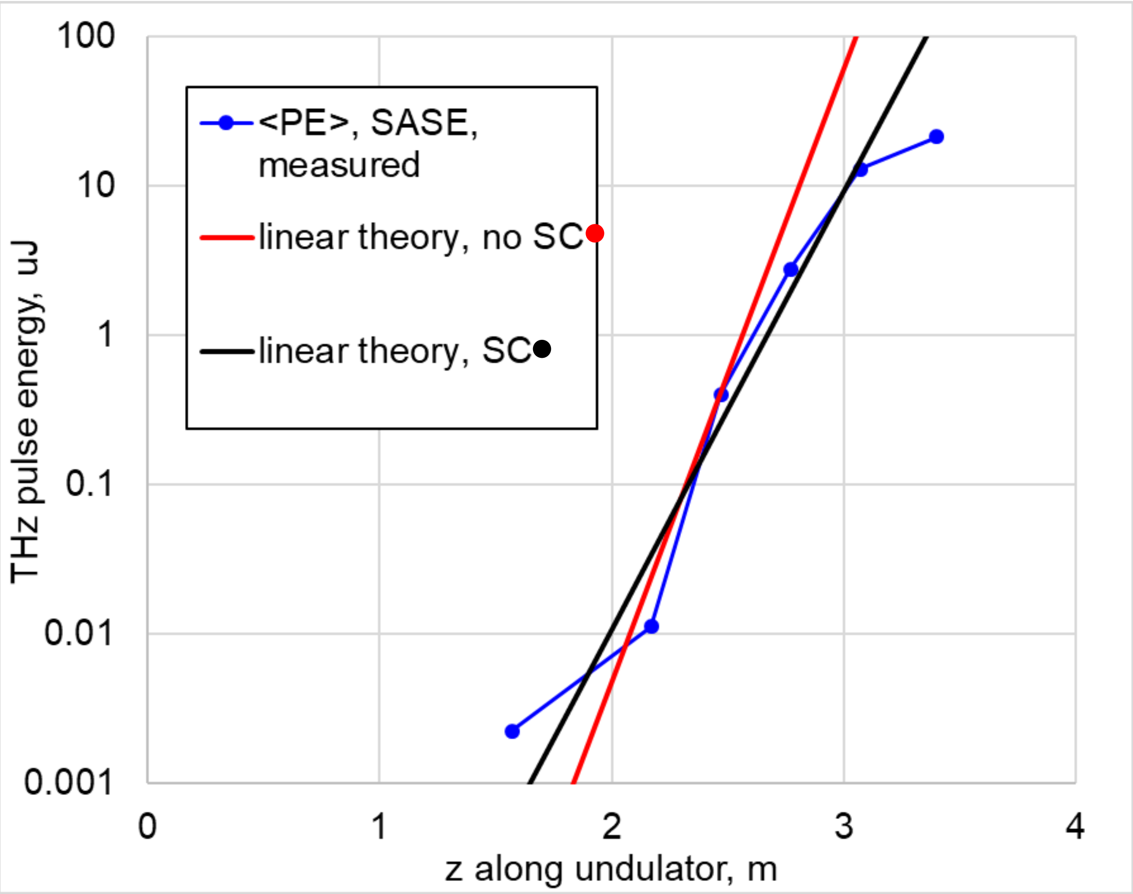

THz FEL Simulations

Challenges → Impact of local bunching factor onto the initial signal

Shot noise in FEL simulations:

- For a **randomly** distribution of electron bunch or bunch slice, the shot noise can be described by $\langle e^{-i\theta_j}\rangle = \frac{1}{n_e}\sum_{j=1}^{n_e} e^{-ikz_j}$, where n_e is number of electrons in the slice (wavelength), so $\left|\langle e^{-i\theta_j}\rangle\right|^2 \sim \frac{1}{n_e}$.
- What if the distribution is **not "fully random"** within the range of the resonant wavelength?
  - ➔ "local" bunching factor: $b_s(z_s) = \frac{\int_{z_s-\lambda/2}^{z_s+\lambda/2} \rho(z) e^{-ikz} dz}{\int_{z_s-\lambda/2}^{z_s+\lambda/2} \rho(z) dz}$,

    z_s is the slice center, $\rho(z)$ is the beam current profile.

    Radiation from one slice = *spontaneous* ($\propto n_e$) + *coherent* ($\propto n_e^2 |b_s|^2$)

$$\frac{coherent}{spontaneous} \propto n_e |b_s|^2$$

	XFEL	THz FEL
Q	1nC	
λ_{rad}	1 nm	100 µm
$k\sigma_z$	$\sim 10^5$	75
$n_e\|b_s\|^2$	$\sim 10^{-8}$	27000

For **Gaussian** current profile

$$b_s(z_s) \cong \frac{z_s}{k\sigma_z^2}\left(\sin(kz_s) - i\cos(kz_s)\right)$$

$$\left|b_{s(z_s)}\right| = \frac{z_s}{k\sigma_z^2}$$

$$\phi_s(z_s) = \tan^{-1}\left(\cot(kz_s)\right)$$

→ $n_e|b_s|^2$ is peaked at $z_s = \pm\sqrt{2}\sigma_z$
→ $n_e|b_s|^2 > 1$, coherent emission dominates
→ $n_e|b_s|^2 < 1$, spontaneous emission dominates

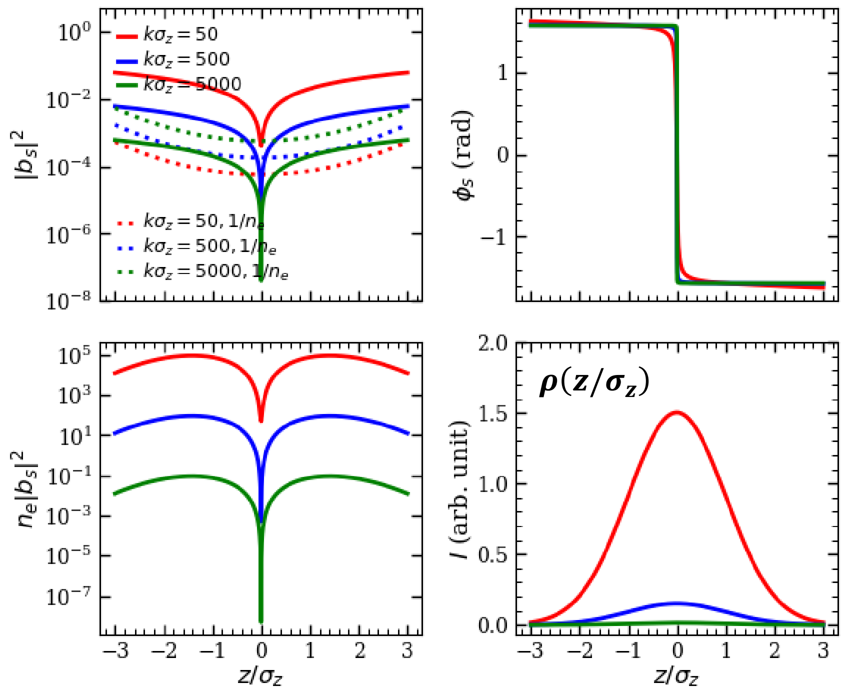

Courtesy X.-K. Li

THz FEL Simulations

Impact of the start conditions - benchmark

Electron beam: 17 MeV/c ($\lambda_s = 100\ \mu m$), **1 pC, 0.3 A**

- One4one = **False**, quiet loading*, Nm = 26*32768 = **851,968** (macropartciles)
- One4one = **True**, **Ne = 6,241,509** (real number of electrons)
- One4one = **False**, smoothed profile, Nm = 26*32768 = **851,968** (macropartciles)

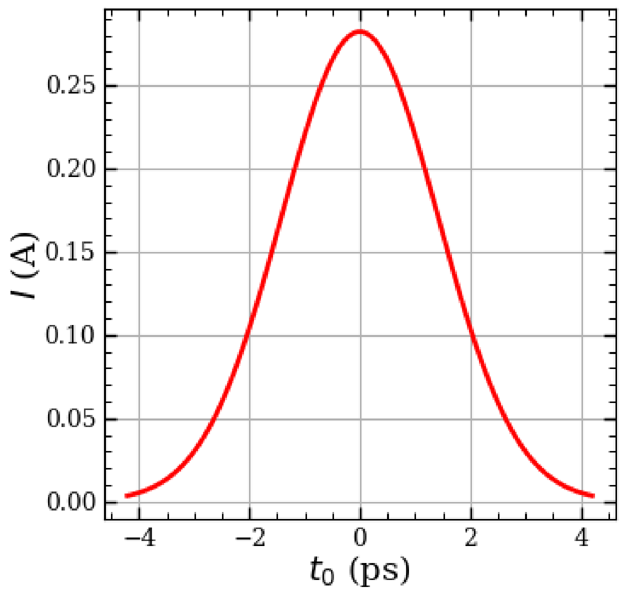

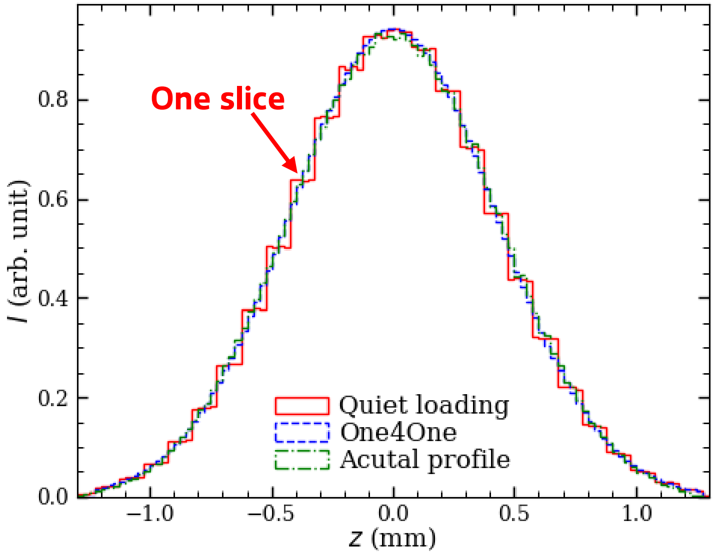

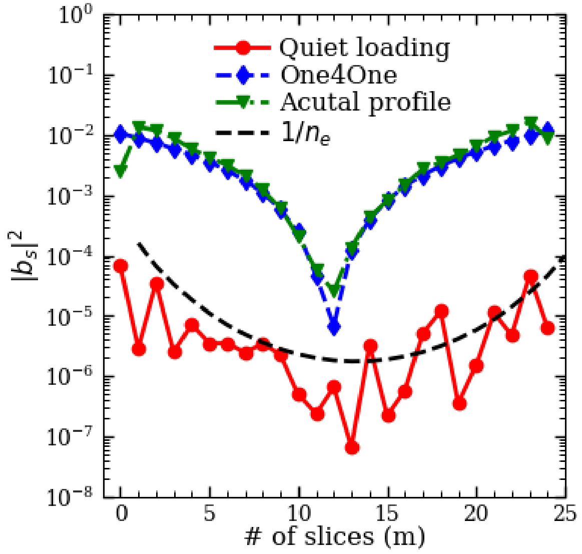

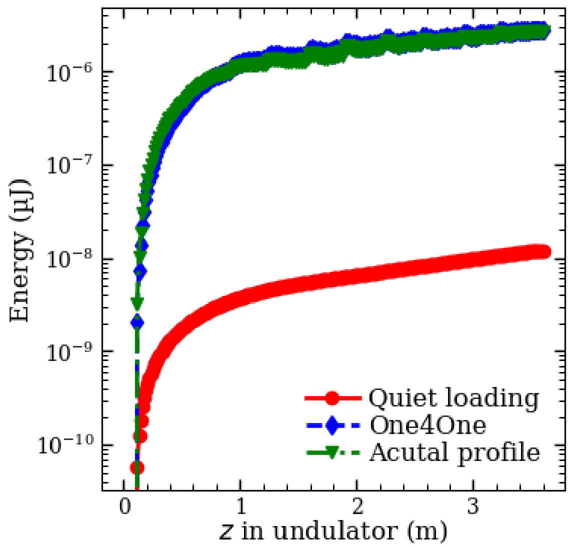

*quiet loading = accurate reproduction of real shot noise based on a step-like slice profile

Courtesy X.-K. Li

THz FEL at PITZ Simulations

Using input from start-to-end simulation

TABLE II. Comparison of THz pusle properties.

Parameters	case I	case II	Units
Current profile in slice	actual	random	
Peack power	923.77 ± 6.87	644.24 ± 98.66	MW
Pulse energy	308.14 ± 2.29	214.89 ± 32.91	µJ
Center wavelength	98.88 ± 0.09	100.76 ± 0.59	µm
Spectral width	1.95 ± 0.08	2.47 ± 0.49	µm
Pulse duration	5.38 ± 0.04	6.21 ± 0.70	ps
Arrival time jitter	0.10	1.30	ps

Electron beam: 17 MeV/c ($\lambda_s = 100$ µm), **2 nC, 112 A**

- One4one = **False**, smoothed profile, Nm = 26*32768 = **851,968**mp
- One4one = **False**, quiet loading, Nm = 26*32768 = **851,968**mp

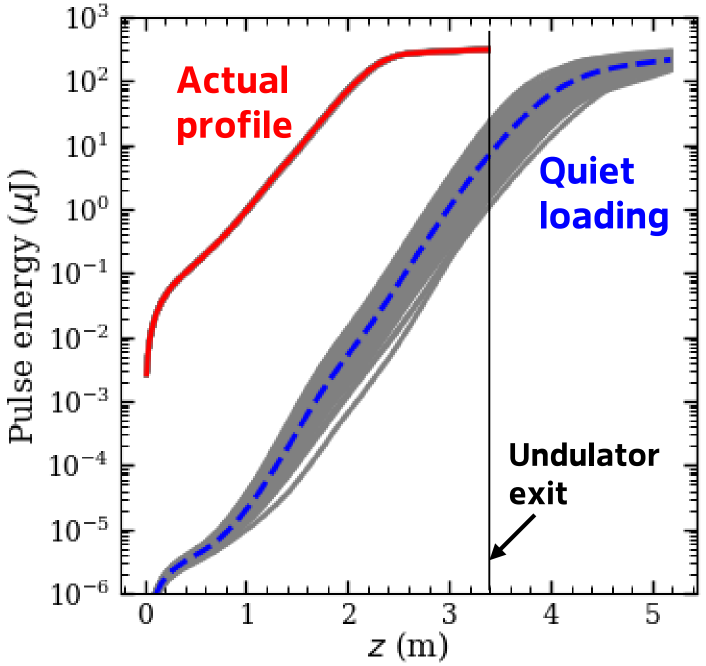

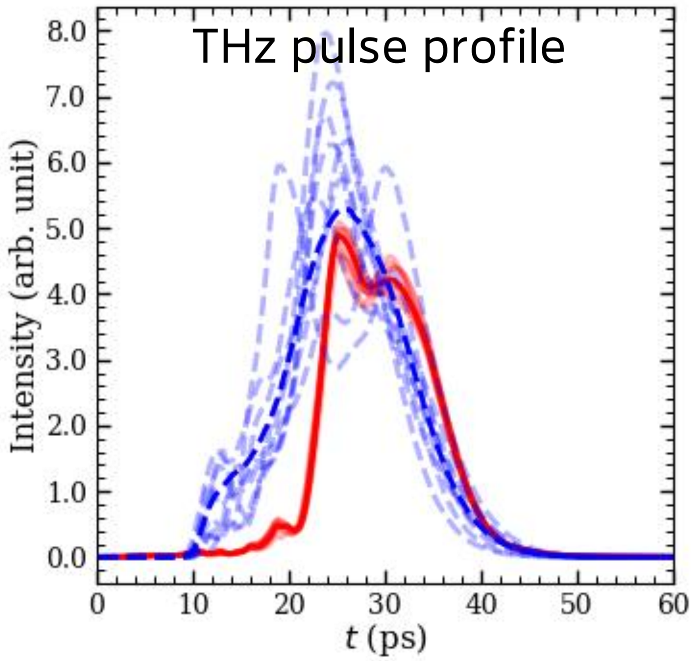

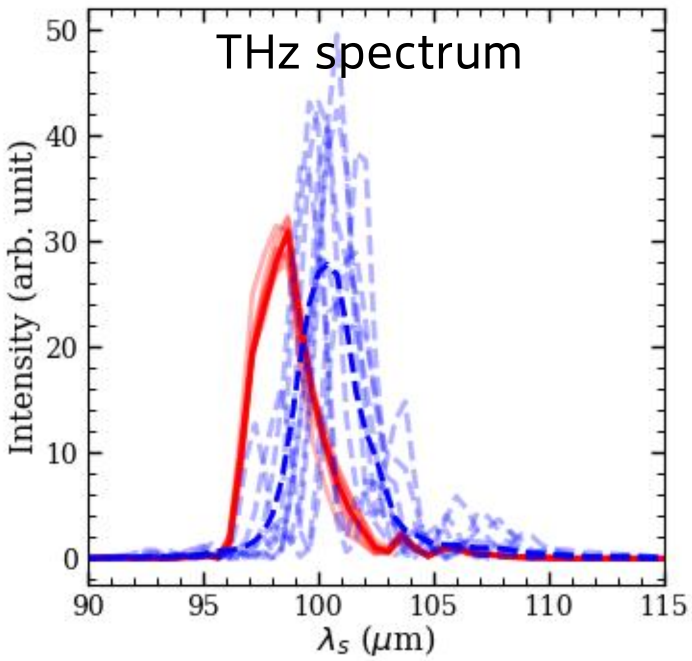

Courtesy X.-K. Li

THz FEL at PITZ: Simulations vs measurements

Using input from start-to-end simulation

- The measured pulse energy was about 40-50 μJ for 2 nC; considering transmission loss of 50%, about 100 μJ has been generated
- From simulations:
  - actual profile → 300-500 μJ
  - quiet loading → only several μJ

Possible reasons: beam trajectory (due to undulator transverse gradient + focusing), space charge, wakefields, waveguide, etc.

Simulated THz pulse profile and spectrum along the undulator

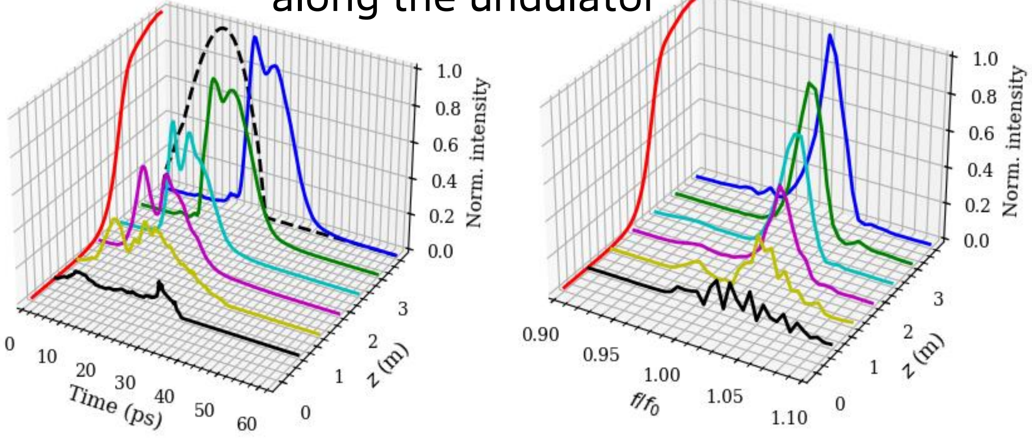

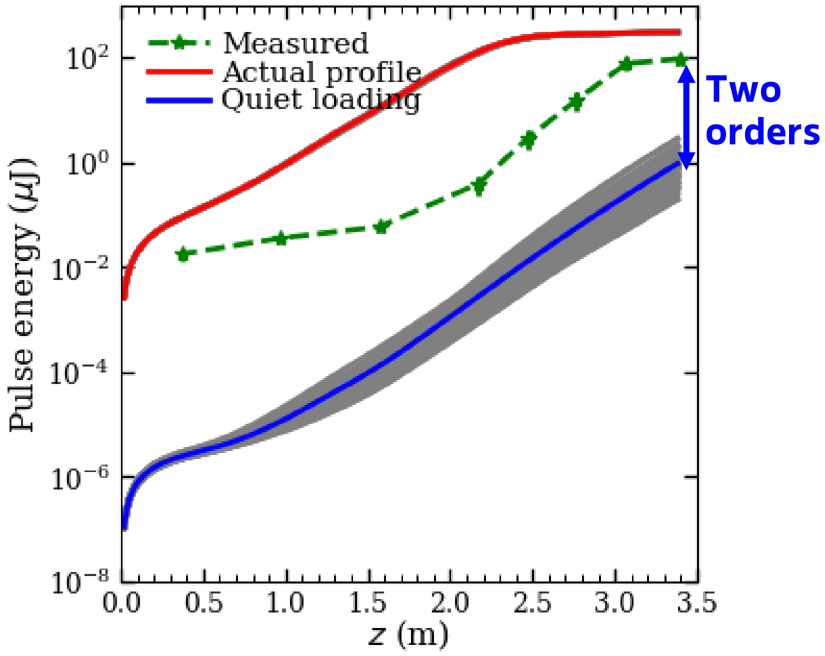

Spectrum from measurement and simulations

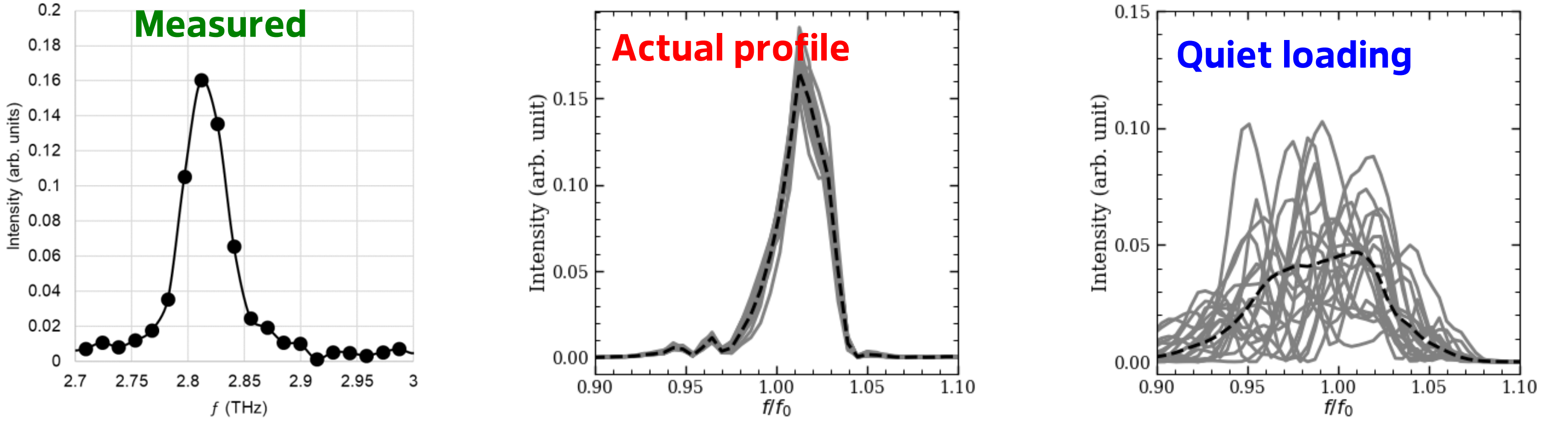

M. Krasilnikov, et al., Phys. Rev. Accel. Beams., 28(3):030701, 2025

THz FEL at PITZ

Conclusions and Outlook

- PITZ has demonstrated strong potential as an accelerator-based THz source by utilizing *high-brightness, high charge electron* bunches optimized for **single-pass, high-gain THz FEL operation** - achieving lasing at 3 THz with **~100 µJ** pulse energy and **<2%** bandwidth - fully compatible with the European XFEL *pulse train structure*
- Ongoing research focuses on demonstrating *tunable* THz generation and performing *detailed characterization* by employing advanced photocathode laser pulse shaping and bunch compression to enhance THz output
- Operational experience and modeling advances are driving the development of an optimized THz source *("ideal" machine*) design aligned with user requirements

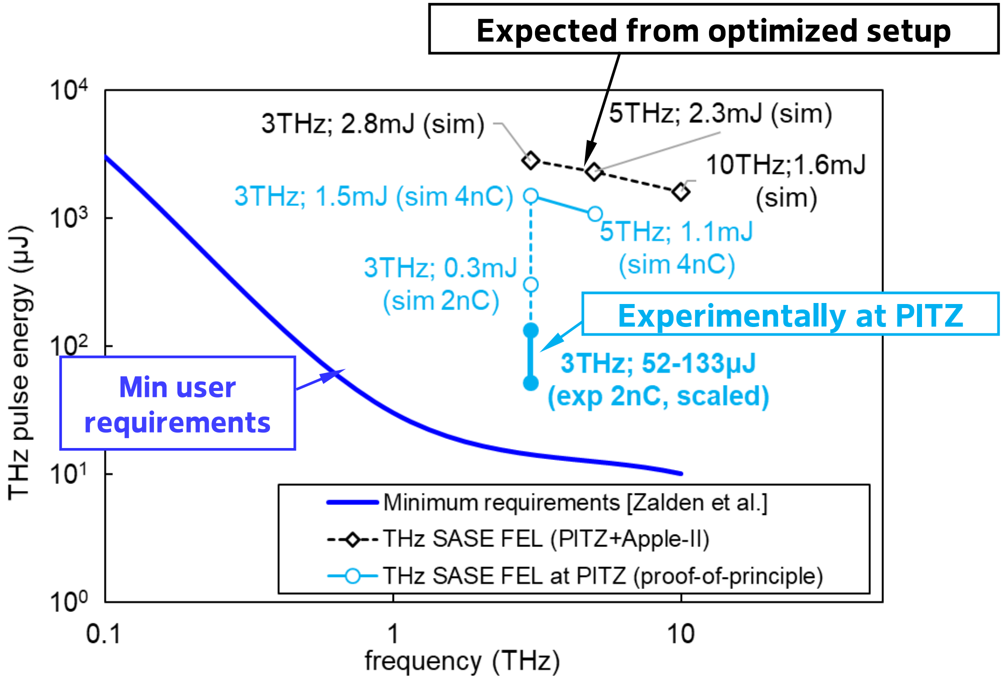

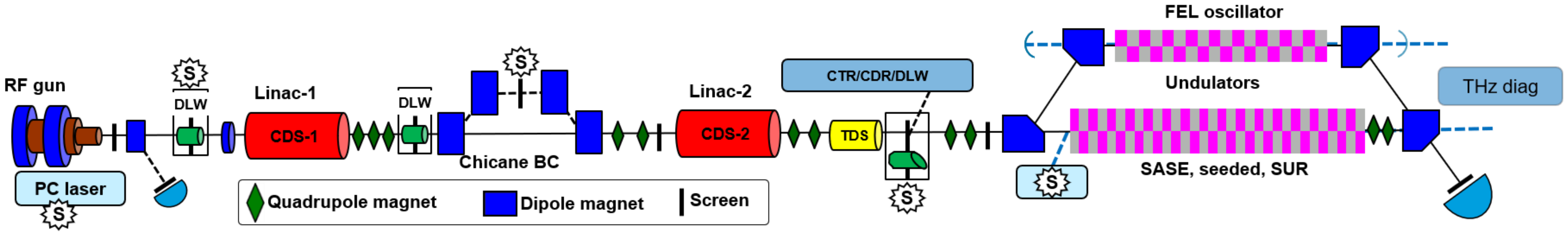

Accelerator-based THz sources

Conclusions and Outlook

Conclusions and Outlook

Accelerator-based THz sources

- Ultra-intense, narrow-/broadband, and tunable **THz radiation** is essential to advance spectroscopy, imaging, and materials research beyond the limitations of conventional sources
- **Accelerator-based** THz sources (CTR/CDR, FEL, …) enable radiation in the “THz gap”:
  - High peak power THz pulses
  - Broadband or tunable narrowband output depending on method
- **THz FELs** offer tunable, high-power, and coherent THz radiation → different operating modes:
  - Oscillator FELs: stable and narrowband
  - Superradiant THz emission: intense broadband bursts from short bunches
  - Single-pass FELs: high peak power
- Key **components**:
  - Electron accelerators
  - Undulators and resonators
  - Bunch compression, precise timing, and diagnostics
- THz FEL **simulations** are challenged by the need to accurately model long wavelengths, shot noise, slippage, and collective effects within large, high-resolution computational domains

IR and THz FEL Facilities

Facility Name	Location	Wavelength range	Type	Accelerator
CLIO	LURE-Orsay, France	3 – 120 μm	Oscillator	NC Linac
FELBE / TELBE	FZ Rossendorf, Germany	4 – 250 μm / 100 – 3000 μm	Oscillator / Superradiant	SC Linac
FHI FEL	Fritz Haber Institute, Germany	3 – 60 μm	Oscillator	NC Linac
FLASH THz Beamline	DESY, Germany	10 – 300 μm	Superradiant	SC Linac
PITZ THz SASE FEL	DESY, Germany	10 – 3000 μm	SASE	SC Linac
SABINA THz/IR FEL	SPARC Laboratory, Italy	10 – 100 μm	SASE	NC Linac
FELIX	Radboud U. Netherlands	3 – 1500 μm	Oscillator	NC Linac
TARLA	Gölbasi, Turky	2.5 – 250 μm	Oscillator	SC Linac
ALICE	Daresbury Lab., UK	4 –16 μm	Oscillator	SC Linac
FELiChEM	NSRL Hefei, China	2 – 200 μm	Oscillator	NC Linac
CAEP THz FEL	CAEP, Mianyang, China	71.4 – 447 μm / 686, 1344 μm	Oscillator /Superradiant	SC Linac
FEL-SUT	SUT, Japan	5 – 16 μm	Oscillator	NC Linac
FEL-TUS	Tokyo University of Science, Japan	5 – 1000 μm	Oscillator	NC Linac
iFEL	Osaka U., Japan	0.23 – 100 μm	Oscillator	NC Linac
KU FEL / THz CUR	Kyoto University, Japan	3.4 – 26 μm / 500 – 1873 μm	Oscillator / Superradiant	NC Linac
LEBRA	Nihon University, Japan	1– 6 μm	Oscillator	NC Linac
t-ACTS	Tohoku U., Japan	180 – 360 μm	Superradiant	NC Linac
NovoFEL	BINP Novosibirsk, Russia	8 – 340 μm	Oscillator	NC ERL
NSRRC THz FEL	NSRRC, Taiwan	214 – 500 μm	Superradiant	NC Linac
PCELL MIR FEL / THz FEL	CMU, Thailand	9.5 – 16.6 μm / 100 – 300 μm	Oscillator / Superradiant	NC Linac
ITST (UCSB FEL)	UCSB, USA	30 – 2500 μm	Oscillator	Electrostatic
Jlab FEL	Jefferson Laboratory, USA	1.5 – 14 μm	Ocillator	SC ERL

W.-K. Lau "THz Free Electron Lasers and Their Applications", ISBA24, Nov.,2024, Chang Mai

Thank you for your attention!